Experimental neuroprotective therapeutics in animal models of Huntington's disease and Parkinson's disease

Ph.D. thesis

Gabriella Gárdián, M.D.

Department of Neurology
University of Szeged
Albert Szent-Györgyi Medical and Pharmaceutical Center
Faculty of Medicine

Szeged
2006

Original papers related to the Ph.D. thesis

I. Klivényi P, Ferrante RJ, **Gárdián G,** Browne S, Chabrier PE, Beal MF (2003) Increased survival and neuroprotective effects of BN82451 in transgenic mouse model of Huntington's disease.
Journal of Neurochemistry 86: 267-272. (Impact factor: 4.825)

II. **Gárdián G,** Yang L, Cleren C, Calingasan NY, Klivényi P, Beal MF (2004) Neuroprotective effects of Phenylbutyrate against MPTP neurotoxicity.
Neuromolecular Medicine 5(3):235-42. (Impact factor: 3.472)

III. **Gárdián G,** Vécsei L (2004) Huntington's disease: pathomechanism and therapeutic perspectives.
Journal of Neural Transmission 111: 1485-1494. (Impact factor: 2.512)

IV. **Gárdián G,** Browne SE, Choi DK, Klivényi P, Gregorio J, Kubilus JK, Ryu H, Langley B, Ratan RR, Ferrante RJ, Beal MF (2005) Neuroprotective effects of Phenylbutyrate in the N171-82Q transgenic mouse model of Huntington's disease.
Journal of Biological Chemistry 280(1): 556-63. (Impact factor: 6.482)

Original papers and abstracts connected to the Ph.D. thesis

I. **Gárdián G,** Vécsei L (1999) Újabb adatok a neurodegeneráció pathomechanizmusához. (Recent data on pathomechanism of neurodegeneration) Topographic Neurology. Conference of Hungarian Neurologists and Psychiatrists Association, Budapest, 1999. *Ideggyógyászati Szemle/Clinical Neuroscience* 52: 247-250.

II. **Gárdián G,** Vécsei L (2000) Neuroprotekció: 2000. (Neuroprotection 2000.) A Magyar Tudományos Parkinson Társaság Konferenciája, Budapest, 2000. Absztrakt könyv pp: 48-52.

III. **Gárdián G,** Vécsei L (2000) Parkinson kór pathomechanizmusa. (Pathomechanism of Parkinson's disease) *Hippokratész* 6: 346-348.

IV. **Gárdián G,** Vécsei L (2002) Neurodegeneráció és neuroregeneráció. A jelen lehetőségei és a közeljövő reményei. Kortünet vagy kórtünet? Mentális zavarok az időskorban. Szerk.: Tariska Péter. Medicina Könyvkiadó Rt., Budapest, p.: 179-189.

V. Jakab K, **Gárdián G,** Endreffy E, Kalmár T, Bachrati Cs, Vécsei L, Raskó I (1999) Analysis of CAG repeat expansion in Huntington's disease gene (IT 15) in Hungarian population. *Eur. Neurol.* 41: 107-110. [IF: 1.379]

VI. Jakab K, **Gárdián G,** Kalmár T, Endreffy E, Vécsei L, Raskó I (1999) Huntington-kóros betegek molekuláris genetikai vizsgálata hazánkban. *Gyermekgyógyászat* 52: 43-47.

VII. Klivényi P, **Gárdián G,** Calingasam NY, Yang L, Beal MF (2003) Additive neuroprotective effects of creatine and a cyclooxygenase 2 inhibitor against dopamine depletion in the 1-methyl-4-phenyl-1,2,3,6-tetrahydropyridine (MPTP) mouse model of Parkinson's disease. *Journal of Molecular Neuroscience* 21: 191-198. [IF: 2.812]

VIII. Klivényi P, **Gárdián G,** Yang L, von Borstel R, Saydoff J, Browne SE, Beal MF (2004) Neuroprotective effects of oral administration of triacetyluridine against MPTP neuro-toxicity. *Neuromolecular Med.* 6: 87-92. [IF: 4.548]

IX. Klivényi P, Siwek D, **Gárdián G,** Yang L, Starkov A, Cleren C, Ferrante RJ, Kowall NW, Abeliovich A, Beal MF (2006) Mice lacking alpha-synuclein are resistant to mitochondrial toxins. *Neurobiol. Dis.* 21: 541-8. [IF: 4.048]

X. Vécsei L, **Gárdián G,** Klivényi P (1997) Experimental models of Huntington's disease: therapeutic strategies. *Eur. J. Neurol.* 4(S1):S29.

List of abbreviations

ATP	adenosine triphosphate
CAG	cytosine-adenine-guanine trinucleotide
CBP	CREBP-binding protein
CREBP	cAMP response element-binding protein
DNA	deoxyribonucleic acid
DOPAC	3,4-dihydroxyphenylacetic acid
GABA	γ-amino-butyric acid
H2A, H2B, H3, H4	histones
HAT	histone acetyltransferase
HD	Huntington's disease
HDAC	histone deacetylase
HVA	homovanillic acid
IT-15	interesting transcript 15
LBs	Lewy bodies
MPTP	1-methyl-4-phenyl-1,2,3,6-tetrahydropyridine
MPP^+	1-methyl-4-phenylpyridinium ion
NADP/NADPH	ox/red nicotinamide-adenine-dinucleotide phosphate
NMDA	*N*-methyl-*D*-aspartate
3-NP	3-nitropropionic acid
PBS	phosphate-buffered saline
PCR	polymerase chain reaction
PD	Parkinson's disease
RNA	ribonucleic acid
RT-PCR	real-time polymerase chain reaction
SAHA	suberoylanilide hydroxamic acid
SNpc	substantia nigra pars compacta
TH	tyrosine hydroxylase

Table of contents

Experimental neuroprotective therapeutics in animal models of Huntington's disease and Parkinson's disease

I. INTRODUCTION

I.1. Huntington's disease

I.1.1. Clinical features

Huntington's disease (HD) is an autosomal dominantly inherited progressive neuro-degenerative disorder. The main symptoms are choreiform, involuntary movements, personality changes and dementia (Garron, 1973). The symptoms usually appear in mid-life and the progression of the disease inevitably leads to death within 15-20 years.

HD is a member of a group of diseases caused by cytosine-adenine-guanine (CAG) repeat expansions, which includes spinocerebellar ataxias, spinobulbar muscular atrophy (X-linked), and dentatorubral-pallidoluysian atrophy.

I.1.2. Neuropathology

The characteristic neuropathological features of HD are macroscopic atrophy of the caudate nucleus, neuronal loss and fibrillary astrogliosis in the striatum. The neuronal loss is selective for medium-sized spiny projection neurons containing GABA/enkephalin and GABA/substance P. The large interneurons (containing NADPH diaphorase, somatostatin, neuropeptide Y) and the large cholinergic neurons remain intact (McGeer et al., 1976; Ferrante et al., 1985; Reiner et al., 1988). The mechanism of selective neuronal loss is un-known. Other areas of intense cell loss and fibrillary astrogliosis include the two segments of the globus pallidus, the substantia nigra pars reticulata, the subthalamic nucleus and several thalamic nuclei. They belong to the basal ganglia circuitry and are connected to the striatum. There is a loss of cortical volume, particularly in cases with more advanced disease, which affects predominantly the large pyramidal neurons in layers III, V and VI (Hedreen et al., 1991).

I.1.3. Genetics

Tandem trinucleotide repeats are not infrequent in the human genome. Although there are 64 possible trinucleotide sequences, when allowance is made for cyclic permutations $(CAG)_n=(AGC)_n=(GCA)_n$, there are only 10 different trinucleotide repeats. Most of them are known as usefully polymorphic microsatellite markers, but certain repeats show anomalous behavior (CAG/CTG and CCG/GGC). In each case, repeats below a certain length are stable in mitosis and meiosis, while above a certain threshold length the repeats become extremely unstable. These unstable repeats are virtually never transmitted unchanged from parent to child. Both expansions and contractions can occur, but there is a bias towards expansion. The average size change often depends on the sex of the transmitting parent, and on the length of the repeat (Strachan and Read, Human molecular genetics, 1996).

The discovery that human disease can be caused by the large-scale expansion of highly unstable trinucleotide repeats was quite unexpected (Fu et al., 1991). Disorders that display triplet repeat expansion in noncoding regions typically cause a loss of gene function, whereas those that occur in coding regions result in an expanded polyglutamine tract in the protein product, and cause a gain of function mutation; the protein becomes toxic, with or without the loss of its normal function. The development of therapeutics for noncoding disorders has therefore focused on restoring the gene function, whereas the therapy for coding disorders is directed toward ameliorating the consequences of the toxic protein (Di Prospero et al., 2005).

The gene responsible for HD was identified in 1993 (Gusella et al., 1993). The mutant gene causing HD was localized to chromosome 4p16.3 and named interesting transcript 15 (IT-15). Its length is 210 kb, it contains 67 exons and it codes a 348 kD, 3144 aa protein, huntingtin, which is widely distributed in both neurons and extraneuronal tissues. The mutation in HD involves the expansion of a trinucleotide (CAG) repeat encoding glutamine at the 5' end of the coding sequence, resulting in a polyglutamine stretch in the huntingtin protein. In healthy individuals, the CAG repeat number ranges from 9 to 35 (median: 19), while in patients with HD the range is 39-121 (median: 44). There is a borderline zone between normal and abnormal CAG repeat lengths (36-39) because of the incomplete penetrance of the disease phenotype (Huntington's Disease Collab. Res. Group, 1993; Kremer et al., 1994; Rubinsztein et al., 1996). Expansion to >55 repeats causes the juvenile form of

the disease. There is an inverse relationship between the CAG repeat number and the age at onset of the symptoms. The gene of HD displays marked instability, particularly when passed through the male germ line, where expansions tend to occur more frequently than contraction. This is the anticipation phenomenon, where the age at onset tends to decrease in successive generations.

I.1.4. Molecular mechanism

The amino acid sequence of huntingtin has no major homology with any known protein (Petersen et al., 1999). The functions of the normal and mutant proteins are still unknown as concerns their details.

Wild-type huntingtin protein is widely distributed in both neurons and extraneuronal tissues. In the brain, the neurons are enriched in huntingtin as compared with the glial cells (Li et al., 1995). In the human brain, huntingtin is present in the cytoplasm of the neuronal somata, dendrites and axons (Sapp et al., 1997). Wild-type huntingtin may act as a molecular scaffold, regulating several cellular processes, including endocytosis, vesicle transport, excitatory synapses, transcriptional events and the mitochondrial function (Harjes et al., 2003). It is essential during development, as homozygous knock-out mice exhibit embryonic lethality. Huntingtin is required in the postembryonic period too for neuronal survival. The wild-type protein appears to upregulate the transcription of brain-derived neurotrophic factor (Zuccato et al., 2001), and also has an anti-apoptotic effect (Zeitlin et al., 1995). At the cellular level, differences have been found in HD brains: in particular, an abnormal nuclear accumulation of the N-terminal fragments of huntingtin, described as neuronal intranuclear inclusion (DiFiglia et al., 1997).

An expanded polyglutamine stretch leads to a conformational change. Antibodies to expanded stretches of polyglutamine discriminate the normal and mutated forms. Expanded polyglutamine domains in mutant protein are postulated to promote protein-protein interactions, which may occur by a "polar zipper" mechanism dependent on hydrogen bonding (Perutz et al., 1994). There is also evidence that transglutaminase may catalyze the cross-linking of huntingtin to other proteins by creating glutamyl-lysine crosslinks, which can inactivate the enzymatic activities of some proteins. A number of proteins are involved: huntingtin-interacting protein (HIP-1) and huntingtin-associated protein (HAP-1), which have roles in

endocytosis and membrane trafficking; and glyceraldehyde-3-phosphate-dehydrogenase (GAPDH) (Petersen et al., 1999). Huntingtin may modulate synaptic transmission, learning and memory via its interaction with postsynaptic density protein-95, a molecule that interacts with excitatory aminoacid receptors, and synaptic GTPase-activating protein (Sun et al., 2001). Mutant huntingtin changes numerous forms of the gene expression by altering the functions of the transcriptional factors (Walton et al., 2000; Wyttenbach et al., 2001).

I.1.5. Early changes in gene expression

The cell function and lifespan are modulated by alterations in gene expression in response to extracellular stimuli. The acetylation-deacetylation and methylation-demethylation of histones in nucleosomes are important in the regulation of gene expression. The nucleosome, the basic unit of chromatin, is composed of highly conserved core histones (H2A, H2B, H3 and H4) and deoxyribonucleic acid (DNA). The degree of acetylation and deacetylation of histones is controlled by the activities of histone acetyltransferases (HATs) and histone deacetylases (HDACs). The post-translational acetylation of these proteins by HATs is thought to neutralize the positive charge and generate a more open DNA conformation. The deacetylation of histones by HDACs restores the positive charges on the histones and leads to condensation of the nucleosome. Hyperacetylated histones are linked to transcriptionally active domains, whereas hypoacetylated histones are associated with transcriptionally silent domains. As the balance of histone acetylation is controlled by HATs and HDACs, the sequestration and depletion of HATs might be corrected by HDAC inhibition (Luthi-Carter et al., 2000; Krämer et al., 2001; Marks et al., 2001; Chang et al., 2002; Hoshino et al., 2003). While histone acetylation is thought to relax the chromatic structure leading to increased gene transcription, subsequent histone methylation (particularly on lysine 9 of H3) leads to transcriptional repression, assisting the termination of gene transcription (Zhang et al., 2001; Pal et al., 2003; Gui et al., 2004). DNA methyltransferases interact with HDACs (Deplus et al., 2002; Sekimata et al., 2001).

A new avenue for therapy involves the identification of nuclear protein–protein interactions. The level of mutant huntingtin is increased intranuclearly in advance of the disease, because of the impaired clearance of the mutant protein as a consequence of the impaired proteosome function. The mutant huntingtin may bind to other polyglutamine-containing

proteins. Numerous of these are transcriptional factors. Early changes in transcription occur in HD. Although some of these changes might be responses to a perturbed cellular metabolism, mutant huntingtin protein can directly interact with and sequester transcription factors which include p53, the cAMP response element-binding protein (CREBP) binding protein (CBP), $TAF_{II}130$, Sp1 (Shimohata et al., 2000; Sawa, 2001; Bates, 2001). Many of these nuclear factors regulate histone acetylation directly. CBP is particularly important, because the CBP level influences a variety of different transcription factors. Mutant huntingtin sequesters CBP and other coactivators, and thereby alters the histone acetylation and gene expression (Walton et al., 2000; Wyttenbach et al., 2001). The cell loss can be reversed by the overexpression of transcription factors or the use of HDAC inhibitors, which indicates a role for transcriptional dysregulation in HD (McCampbell et al., 2001; Steffan et al., 2001; Dunah et al., 2002; Taylor et al., 2003). HDAC inhibitors have received attention as potential therapeutic drugs for several other diseases, including cancer, hemoglobinopathy and cystic fibrosis. There are 6 classes of HDAC inhibitors, ranging from the very simple short-chain fatty acid butyrate to complicated compounds such as depsipeptide. The specificity of each inhibitor for different HDACs has not been identified (Chang et al., 2002). However, the HDAC inhibitor sodium phenylbutyrate is FDA-approved for the treatment of other disorders, and the fact that its long-term use is associated with only limited toxicity makes it a potential clinical candidate.

I.2. Parkinson's disease

Idiopathic Parkinson's disease (PD) is regarded as the most common neurodegenerative disorder of the aging brain after Alzheimer's dementia. Clinically, it is characterized by resting tremor, bradykinesia, cogwheel rigidity and postural instability. The cardinal biochemical abnormality is the profound deficit in brain dopamine level, which is primarily, but not exclusively, attributed to the loss of neurons of the nigrostriatal dopaminergic pathway. Aside from the loss of dopaminergic and nondopaminergic cell groups, other prominent neuropathological features of PD include gliosis and the presence of intraneuronal proteinaceous inclusions called Lewy bodies (LBs). Although the etiology of PD is incompletely understood, increasing evidence indicates that deficits in mitochondrial function, oxidative and nitrosative stress, inflammatory mechanisms, the accumulation of aberrant or misfolded proteins, and an

ubiquitin-proteasome system dysfunction may be the principal molecular pathways or events that commonly underlie the pathogenesis of PD (Samii et al., 2004; Hague et al., 2005)

I.3. Animal models of Huntington's disease

One research aim is to determine the earliest molecular changes associated with HD. There is no possibility for this in humans, but various early changes have been identified in animal models of HD. They are constructed by an excitotoxin causing striatal lesions, or by mitochondrial toxins inducing energy impairment, or by generating transgenic mice.

I.3.1. Excitotoxin model

The process of glutamate-mediated neuronal death (called excitotoxicity) was discovered about three decades ago (Olney, 1969). There is evidence that excitotoxicity may play a role in the pathogenesis of HD (Coyle et al., 1976; McGeer et al., 1976; DiFiglia, 1990). It has been demonstrated that the injection of quinolinic acid produces a lesion which is a reliable model of HD (Schwarcz et al., 1983; Beal et al., 1986; Vécsei et al., 1991, 1996, 1998). There is an increased vulnerability to N-methyl-D-aspartate (NMDA) receptor agonists in cultured striatal neurons from a different mouse model of HD (Cepade et al., 2001). An impairment of the mitochondrial energy metabolism can result in decreased adenosine triphosphate (ATP) production, with an accompanying reduction of the Na^+, K^+-ATP-ase activity. Partial cell depolarization may occur, leading to alleviation of the voltage-dependent Mg^{2+} blockade of NMDA receptor-associated channels. Accordingly, endogenous levels of glutamate activate NMDA receptors. The concomitant increase in Ca^{2+} influx into the neurons may trigger further free radical production (Beal, 1992; Csillik et al., 2002). Medium spiny neurons are especially affected in HD. These "spines" are rich in excitatory NMDA receptors. The state of phosphorylation of the NMDA receptor subunits enhances their synaptic efficacy so as to favor the appearance of choreiform movements. Mutant huntingtin enhances excitotoxic death in cultured cells via an enhanced NMDA receptor sensitization.

I.3.2. Mitochondrial toxin model

The disruption of the mitochondrial function and the glucose metabolism contributes to neuronal cell death (Beal, 1997). A mitochondrial dysfunction has been implicated in the

pathogenesis of HD, but it could be secondary (Manfredi et al., 2000). Mitochondria are both important targets and important sources of reactive oxygen species. In HD patients, the glucose metabolism is decreased in the affected striatal and cerebral cortex. Defects in the glucose metabolism lead to the generation of free radicals and oxidative damage. Malonate, 3-acetylpyridine and 3-nitropropionic acid (3-NP) could lead to a pattern of striatal atrophy similar to that in HD.

3-NP is an irreversible inhibitor of succinate dehydrogenase that inhibits both the Krebs - Szent-Györgyi cycle and complex II activity of the electron transport chain. Since complex II is an entrance pathway into the electron transport chain, it can reduce ubiquinone (coenzyme Q), an important electron carrier to complex III. 3-NP reduces the cellular levels of ATP and causes neuronal damage by an excitotoxic mechanism (Ludolph et al., 1991, 1992). Lesioning with 3-NP provides an animal model of HD which closely resembles the human disease in both pathology and symptomatology.

I.3.3. Knock-out mouse model

The nullizygous phenotype is embryonic lethal, clearly demonstrating that the HD gene plays an important role in early development (Bates et al., 1997).

I.3.4. Transgenic mouse models

A major step in the study of HD was the creation of a transgenic mouse model. The ideal transgenic mouse model would have a robust phenotype, rapid disease onset and progression, well-defined behavioral abnormalities and neuropathological features that accurately replicate human HD. There are many mouse models of HD, but they fall into 3 broad categories:

(1) mice that express exon-1 fragments of the human huntingtin gene containing CAG repeat expansion mutations in addition to both alleles of murine wild-type huntingtin gene;

(2) mice with pathogenic CAG repeats inserted into the existing CAG expansion in murine huntingtin gene (knock-in mice); and

(3) mice that express the full-length human HD gene in addition to murine huntingtin gene.

The R6/2 mouse model belongs in the first group. It has exon-1 of the human HD gene with an expanded CAG repeat. These mice (line R6/2) have CAG repeat lengths of 141-157 under the control of the human HD promoter. At approximately 6 weeks of age, the R6/2 mice show a loss of body weight, and at 9–11 weeks they develop an irregular gait, stuttering stereotypic movements, resting tremors and epileptic seizures. The mice demonstrate a progressive weight loss and brain atrophy. Neuronal intranuclear inclusions that are immunopositive for huntingtin and ubiquitin are detected in the striatum at 4 weeks. These animals, however, are not a perfect neuropathological match for the human HD pathology. R6/2 mice have a more extensive huntingtin aggregate distribution than is typical of HD and they are resistant to excitotoxicity, which may be related to an increased capacity to process calcium (Mangiarini et al., 1996; Bates et al., 1997).

N171-82Q mice express a cDNA encoding a 171 amino acid N-terminal fragment of huntingtin exon-1 containing 82 CAG repeats which also belongs in the first group (Schilling et al., 1999). The mice develop tremors, a progressive weight loss, incoordination, and abnormal hindlimb clasping by 3-4 months of age, and die prematurely at 4-6 months of age. The animals appear normal for the first 2 months of life, but the initial phenotypic abnormality is the failure to gain weight from 2 months onwards. The striatal N-acetylaspartate concentration is reduced as early as 50 days of age (indicating a neuronal dysfunction), and an abnormal systemic glucose tolerance occurs by 75 days of age (Jenkins et al., 2005). Significant reductions in gene expression include reductions in dopamine D2 receptors, adenosine A2a receptors and adenylyl cyclase (Luthi-Carter et al., 2000). The diffuse nuclear accumulation of huntingtin, rare nuclear aggregates and cytoplasmic aggregates occurs as early as 4 weeks of age (Schilling et al., 1999). There are degenerating neurons as assessed by caspase staining, terminal deoxynucleotidyl transferase-mediated UTP nick end labeling, and electron microscopy (Yu et al., 2003).

Knock-in transgenic mouse models in general have a less robust behavioral phenotype than N-terminal fragment models. However, they are a more precise genetic model of HD.

The YAC (yeast artificial chromosome) mouse model of HD belongs in the third group. These mice express the entire human gene containing 128 CAG repeats and show behavioral abnormalities. These changes correlate with the onset of loss of cortical and striatal neurons (Slow et al., 2003).

I.4. MPTP model of Parkinson's disease

Investigators still rely on experimental models of PD to obtain greater insight into its cause and pathogenesis. Whereas recent genetic discoveries have led to a number of different genetic models of PD, none of these shows the typical degeneration of dopaminergic neurons. Among the various accepted experimental models of PD, neurotoxins have remained the most popular tools with which to produce selective neuronal death in both *in vitro* and *in vivo* systems.

1-Methyl-4-phenyl-1,2,3,4-tetrahydropyridine (MPTP) was discovered in 1982, when a group of drug addicts in Northern California developed the subacute onset of severe parkinsonism. Investigations revealed that the syndrome was caused by the self-administration of a synthetic heroin analog that had been contaminated by a by-product (MPTP) during manufacture. MPTP is a neurotoxin which produces parkinsonian syndrome in both humans and animals. MPTP is highly lipophilic and readily crosses the blood-brain barrier. Pathologic studies reveal severe degeneration in the pars compacta of the substantia nigra after systemic MPTP administration. Studies of the mechanism of MPTP neurotoxicity demonstrated that 1-methyl-4-phenylpyridinium (MPP^+), the major metabolite of MPTP, is responsible for the neuronal injury. MPP^+ formation is catalyzed by monoamine oxidase B in astrocytes. MPP^+ is taken up into dopaminergic neurons by the synaptic dopamine transporter and concentrated in the mitochondria, where it inhibits complex I of the electron transport chain (Tipton et al., 1993). This binding produces an impairment of oxidative phosphorylation, this inhibition correlating well with the neurotoxic effect of MPP^+. The impairment of mitochondrial respiration leads to the enhanced generation of free radicals, the rapid depletion of ATP levels, the accumulation of NADH and lactate, and significant alterations in the cellular Ca^{++} content. MPTP treatment produces intracellular proteinaceous inclusions resembling immature LBs that are filamentous and contain α-synuclein (Forno et al., 1988; Beal, 2001).

II. AIMS OF THE STUDY

1. There is substantial evidence that excitotoxicity and oxidative damage may contribute to the pathogenesis of HD. We set out to whether the novel anti-oxidant, anti-inflammatory compound BN82451 exerts neuroprotective effects in the R6/2 transgenic mouse model of HD.

2. There is evidence that mutant huntingtin interacts with transcription factors, leading to reduced histone acetylation. In different animal models of HD, HDAC inhibitors arrest the ongoing progressive neuronal degeneration. A critical issue is whether a HDAC inhibitor sodium phenylbutyrate exerts neuroprotective effects when administered after the onset of symptoms in the N171-82Q transgenic mouse model of HD.

3. We examined the effects of sodium phenylbutyrate on the gene expression levels and patterns in the N171-82Q transgenic mouse model of HD.

4. We examined whether the administration of sodium phenylbutyrate could result in neuroprotective effects against MPTP neurotoxicity, which has been used to model Parkinson's disease.

III. MATERIALS AND METHODS

III.1. BN82451 experiment – R6/2 model

Animals

Male transgenic HD mice of the R6/2 strain were obtained from Jackson Laboratories (Bar Harbor, ME, USA). Male R6/2 mice were bred locally with females from their background strain (B6CBAFI/J). The offspring were genotyped with a polymerase chain reaction (PCR) assay on the tail DNA. Nine to 10 mice in each group were examined for survival, with equal numbers of males and females in each group. All animal experiments were carried out in accordance with the NIH Guide for the Care and Use of Laboratory animals and were approved by the local animal care committee.

Treatment

At 30 days of age, the mice were fed laboratory chow supplemented with BN82451 at 0.015%, or a standard unsupplemented diet. Assuming an intake of 5 g of chow daily, is equivalent to a dose of 30 mg/kg/day.

Behavior and weight assessment

Motor performance was assessed from 30 days of age in the R6/2 experiments (n=9–10 mice per group) using the rotarod apparatus (Columbus Instruments, Columbus, OH, USA). The mice were tested at 12 rpm. They participated in two trials, and the better result was recorded. They were weighed at the same time, once a week.

Survival

The mice were observed every morning and during the late afternoon. The criteria on for killing was the point in time at which the mice were unable to initiate movement after being gently prodded for 2 min.

Stereology/quantitation

Serial-cut coronal tissuesections beginning from the most rostral segment of the neostriatum to the level of the anterior commissure were used for aggregate analysis.

Unbiased stereologic counts of ubiquitin-positive aggregates (≥1.0 μm) were obtained from the neostriatum in 10 BN82451-treated and 10 unsupplemented diet R6/2 mice at 70 days, using Neurolucida Stereo Investigator software (Microbrightfield, Colchester, VT, USA). The total areas of the neostriatum were defined in serial sections in which counting frames were randomly sampled. The dissector counting method was employed, in which ubiquitin-positive aggregates were counted in an unbiased selection of serial sections in a defined volume of the neostriatum. Striatal neuron areas were analyzed by microscopic videocapture, using a Windows-based image analysis system for area measurement (Optimas, Bioscan Incorporated, Edmonds, WA, USA). This software automatically identifies and measures profiles. Identified cell profiles were manually verified as neurons and exported to Microsoft Excel. Cross-sectional areas were analyzed by using Statview.

Statistics

Data are expressed as means ± standard error of the mean (SEM). Rotarod and weight data were compared by analysis of variance (ANOVA). Survival data were analyzed by the Kaplan–Meier test.

III.2. Sodium phenylbutyrate experiment – N171-82Q model

Animals

Transgenic N171-82Q mice were originally obtained from Drs. Ross and Borchelt (The Johns Hopkins University, Baltimore, MD, USA), and maintained on a B6C3F1 background (Jackson Labs., Bar Harbor, ME, USA). The offspring were genotyped by using a PCR assay on the tail DNA. The mice were housed 4 or 5 per cage, with free access to food and water, under standard conditions with a 12-h light/dark cycle. Male and female N171-82Q mice, and littermates, were equally distributed between experimental groups.

Treatment

The mice received ip injections of sodium phenylbutyrate (100 mg/kg/day, volume: 3.33 ml/kg; Triple Crown USA, Inc., Perkasie, PA, USA) or vehicle (phosphate-buffered saline (PBS): 3.33 ml/kg), 6 days per week from 75 days of age.

Survival

Thirty-six mice (24 in the drug group and 12 in the vehicle group) were used in survival, weight and behavior studies. They were observed daily, and were deemed to have reached the end-stage of the disorder when they could no longer initiate movement after being gently agitated for 2 min. Death was recorded when the animals reached this stage and were euthanized with a Na-pentobarbital overdose, or at the time of natural death if this occurred between daily inspections.

Behavioral and Weight Assessment

Motor performance was assessed by using an accelerating rotarod apparatus (Columbus Instruments, Columbus, OH, USA). The rotarod was accelerated from 0 rpm at a rate of 5.3 rpm/min over 180 s, and then maintained at 16 rpm for a further 120 s (300 s total). The time elapsed on the rotarod measures the mouse's motor competency in the task. The mice were given two rotarod training sessions to accustom them to the apparatus, and they were then tested twice weekly from 75 days of age. Each mouse participated in three 300-s trials per test session, with the best result recorded. The animals were weighed twice a week.

Histone Acetylation and Methylation Levels in Brain Tissue

Fifteen N171-82Q and littermate wild-type mice (aged 4-5 months) received single ip injections of 100 mg/kg sodium phenylbutyrate in PBS, or the vehicle alone (PBS). Mice were sacrificed at 0, 1, 2, 3 and 4 h post-injection (n=3 per group), and the brains and spleens were harvested and immediately frozen in liquid nitrogen. Nuclear fractionation was carried out according to the Ausubel protocol (Ausubel et al., 2000). Levels of acetylated H3 were measured by Western blot analysis according to published methods (anti-acetylated H3 dilution 1:3000; anti-acetylated H4 dilution 1:2000) (Warrell et al., 1998). Levels were compared with butyrate-treated and untreated HeLa cell extracts. Histone methylation in both vehicle and sodium phenylbutyrate-treated wild-type and N171-82Q mice at 0, 1, 2 and 3 h was measured by Western blot analysis, using an anti-dimethylated H3 (Lys9) antibody (Upstate Biotechnology, Lake Placid, NY, USA). Anti-acetylated H3 and H4 antibodies and also butyrate-treated and control HeLa cell extracts were obtained from Upstate Biotechnology (Lake Placid, NY, USA), and anti-rabbit IG HRP was from Amersham Biosciences (Piscataway, NJ, USA). The Western blots were quantitated by using computer-assisted densitometry.

Histology and Immunohistochemical Localization of Acetylated and Methylated Histones

The mice were treated with 100 mg/kg sodium phenylbutyrate or PBS from 75 days of age. At 100 or 120 days of age, the animals were deeply anesthetized and transcardially perfused with 4% paraformaldehyde (n=5 per group). The brains were removed, post-fixed with the perfusant for 2 h, and then cryoprotected in 20% glycerol/2% DMSO. The brains were then cut into frozen 50-μm thick sections, and serial sections were stained for Nissl substance (cresyl violet) or immunostained with an antibody recognizing the first 256 amino acids of human huntingtin (EM48, dilution: 1:1000). An antibody to ubiquitin (dilution: 1:200, Dako Corporation, Carpintena, CA, USA) was also used to confirm the presence of protein aggregates. Immunocytochemical localization of acetylated H3 and acetylated H4 was conducted in adjacent sections, as previously described (Richon et al., 2000). Immunocytochemical detection of histone methylation was performed with an antibody to anti-dimethyl-histone H3 (Lys9) (Upstate Biotechnology, Lake Placid, NY, USA). Caspase activation was examined by using an affinity-purified anti-active caspase 3 antibody (dilution: 1:1000, Pharmingen, San Diego, CA, USA).

Stereology/Quantitation

Serial-cut coronal tissue sections beginning from the most rostral segment of the neostriatum to the level of the anterior commissure were used for huntingtin aggregate analysis. Unbiased stereologic counts of huntingtin-positive aggregates (≥1.0 μm in diameter) were obtained from the dorsomedial neostriatum in 5 mice each from sodium phenylbutyrate-treated and PBS-treated N171-82Q mice at 100 and 120 days, using Neurolucida Stereo Investigator software (Microbrightfield, Colchester, VT, USA). The total areas of the rostral neostriatum were defined in serial sections in which counting frames were randomly sampled. The optical dissector method was employed with estimation of the number of huntingtin-positive aggregates. Striatal neuron areas were analyzed by microscopic videocapture, using a Windows-based image analysis system for area measurement (Optimas, Bioscan Incorporated, Edmonds, WA, USA). The software automatically identifies and measures profiles. All computer-identified cell profiles were manually verified as neurons and exported to Microsoft Excel. Cross-sectional areas were analyzed, using Statview.

III.3. Sodium phenylbutyrate experiment – N171-82Q model, gene expression

RNA Isolation and Microarray Analysis

Striata were dissected from mouse brains and immediately frozen in liquid nitrogen. Total RNA was isolated by extraction with TRIzol (Invitrogen, Carlsbad, CA, USA). Labeled cRNA probes were generated from total RNA samples by using the Message-Amp™ cRNA kit (Ambion Inc., Austin, TX, USA). Briefly, the procedure consists in the reverse transcription of 2 μg of total RNA with a T7 oligo(dT) primer bearing a T7 promoter sequence, followed by *in vitro* transcription of the resulting DNA with T7 RNA polymerase to generate antisense RNA copies of each mRNA. The qualities of the total RNA and labeled cRNA were assessed with Agilent's Lab-on-a-Chip total RNA nano-biosizing assay (Agilent Technologies, Palo Alto, CA, USA). Biotinylated cRNA probes were hybridized to Murine Genome Array U74Av2 chips, containing 6000 identified genes and 6000 EST clusters, using the Affymetrix Fluidics Station 400 according to the manufacturer's standard protocol. The image data on each individual microarray chip were scaled to 250 target intensity, using the Microarray Suite software (Affymetrix, Santa Clara, CA, USA). Drug-induced alterations in gene expression were analyzed by using the GeneSpring software (Silicon Genetics, Redwood, CA, USA). Data analysis was carried out on 10 microarrays (5 PBS-treated and 5 sodium phenylbutyrate-treated mice). Normalization was carried out by using default normalization parameters with GeneSpring software as follows: per sample, by dividing the raw data by the 50th percentile of all measurements, and per gene, by dividing the raw data by the median of the expression level for specific samples. Data from probe sets representing genes that failed the detection criteria (labeled "Absent" or "Marginal" in all 10 microarrays) were eliminated, and all further analyses were carried out on the remaining 7116 probe sets. The Welch t-test statistical method was used to find differentially expressed genes by two-group comparisons, and genes were assumed to be significantly upregulated or downregulated if the calculated p value was <0.05.

Real-time RT–PCR

One-step quantitative real-time RT–PCR using a LightCycler thermal cycler system (Roche, Indianapolis, IN, USA) was performed to confirm microarray results. PCR was carried out with the SYBR Green quantitative RT-PCR system (Sigma, St. Louis, MO, USA)

and gene-specific primers for 40 cycles according to the manufacturer's protocols. After amplification, melting curve analysis and length verification by gel electrophoresis were carried out to confirm the specificity of PCR products. As a negative control, template RNA was replaced with PCR-grade water. Calculations of threshold cycle and difference were analyzed with the LightCycler analysis software (Roche, Indianapolis, IN, USA). Gene-specific primers were designed by using LightCycler probe design software (Roche, Indianapolis, IN, USA). The PCR primer pairs used for each gene were as follows:

Gfer, 5'-GCCTGCACAATGAGGT-3' and 5'-GGCTCAGATGCACTTTAAT-3';
Gstm3, 5'CTCTGCCTACATGAAGAG-3' and 5'-GGAGAGAGAACCGGGA-3';
Psma3, 5'-CATTAGCAGACATAGCGAG-3' and 5'-ATCACGGCAAGTCATTT-3';
Casp9, 5'-AGAACGACCTGACTGC-3' and 5'-CTCCCGTTGAAGATATTCAC-3';
Cflar, 5'-TGGAATACCGTGACAGTC-3' and 5'-CTTGCATATCGGCGAAC-3';
Prkce, 5'-AAACACCCTTATCTAACCCA-3' and 5'-AGATCACTCCGTGCTG-3'; and
GAPDH, 5'-AGAGCTGAACGGGAAG-3' and 5'-GTTGAAGTCGCAGGAG-3'.

Data Analysis

Data are expressed as means ± SEM. Statistical comparisons of rotarod, weight data, bioassay and histological data were performed by ANOVA or repeated measures ANOVA. Survival data were analyzed by using Kaplan-Meier survival curves and the Mantel-Cox log-rank test.

III.4. Sodium phenylbutyrate experiment – MPTP model

MPTP Model

Three-month-old Swiss-Webster mice were purchased from Jackson Labs, Bar Harbor, ME, USA. They were housed in a room maintained at 20–22 °C on a 12-h light/dark cycle with food and water available *ad libitum*. Sodium phenylbutyrate (250 mg/kg) or vehicle (PBS) was administered 1 day before and for 7 days following MPTP administration. MPTP was administered to the mice ip four times at a dose of 20 mg/kg at 2-h intervals. The animals were sacrificed 1 week later and the striata were dissected. Twelve mice were examined in each group.

HPLC Assay for Catecholamines

The dissected striata were sonicated and centrifuged in chilled 0.1 M perchloric acid (~100 μL/mg tissue). The supernatants were taken for measurements of dopamine and its metabolites 3,4-dihydroxyphenylacetic acid (DOPAC) and homovanillic acid (HVA), by HPLC as modified from a previously described method (Beal et al., 1990, 1992).

1-Methyl-4-Phenylpyridinium (MPP^+) Levels

MPTP (20 mg/kg) was administered ip four times at 2-h intervals. The animals were killed 90 min after the last injection. MPP^+ levels were quantified by HPLC, with UV detection at 295 nm. Samples were sonicated in 0.1 M perchloric acid and an aliquot of supernatant was injected onto a Brownlee Aquapore X 03-224 cation-exchange column (Rainin, Woburn, MA, USA). Samples were eluted isocratically with 90% 0.1 mM acetic acid and 75 mM triethylamine HCl, pH 2.3, adjusted with formic acid and 10% acetonitrile.

Histological Analysis

The mice were anesthetized with sodium pentobarbital and perfused transcardially with 0.1 M PBS (pH 7.4), followed by 4% paraformaldehyde in 0.1 M PBS (pH 7.4). The brains were removed, postfixed for 2 h in the same fixative, and then placed in 30% sucrose overnight at 4 °C. For MPTP-lesioned brains, serial coronal sections (50 μm) were cut through the substantia nigra. Two sets consisting of 8 sections each, 100 μm apart, were prepared. One set of sections was used for Nissl staining (cresyl violet). The other set was processed for tyrosine hydroxylase (TH) immunohistochemistry, using the avidin–biotin–peroxidase technique. Briefly, free-floating sections were pretreated with 3% H_2O_2 in PBS for 30 min. The sections were incubated sequentially in

(a) 1% bovine serum albumin (BSA)/0.2% Triton X-100 for 30 min,

(b) rabbit anti-TH affinity-purified antibody (Chemicon, Temecula, CA, USA; 1:2000 in PBS/0.5% BSA) for 18 h,

(c) biotinylated anti-rabbit IgG (Vector Laboratories, Burlingame, CA, USA; 1:500 in PBS/0.5% BSA) for 1 h, and

(d) avidin–biotin–peroxidase complex (Vector; 1:500 in PBS) for 1 h.

The immunoreaction was visualized by using 3,3'-diaminobenzidine tetrahydrochloride dehydrate with nickel intensification (Vector) as the chromogen. All incubations and rinses were performed with agitation, using an orbital shaker at room temperature. The sections were mounted onto gelatin-coated slides, dehydrated, cleared in xylene, and coverslipped. The numbers of Nissl-stained or TH-immunoreactive cells in the substantia nigra pars compacta (SNpc) were counted by using the optical fractionator method in the Stereo Investigator (v. 4.35) software program (Microbrightfield, Burlington, VT, USA).

Statistical Analysis

Data are expressed as means ± SEM. Statistical analysis was performed by using one-way ANOVA followed by the Newman–Keuls *post hoc* test. The Mann–Whitney U-test and Student's t-test were used to analyze differences in lesion volumes.

IV. RESULTS

IV.1. BN82451 experiment – R6/2 model

Administration of BN82451 in the diet resulted in a significant improvement in the survival of R6/2 mice as compared with that of the mice fed an unsupplemented diet (Figure 1a). The controls deteriorated at 57 days and the treated mice at 72 days of age which is consistent with a delay in disease onset. The mean survival increased from 92.6±3.5 days to 106.8 ± 1.1 days with BN82451 ($p < 0.001$). The survival was extended by 14 days (15.3%). The treated mice had a significantly better motor performance from 57 to 67 days of age than that of the mice fed an unsupplemented diet (Figure 1b). This finding was replicated in other groups of control and BN82451-treated mice.

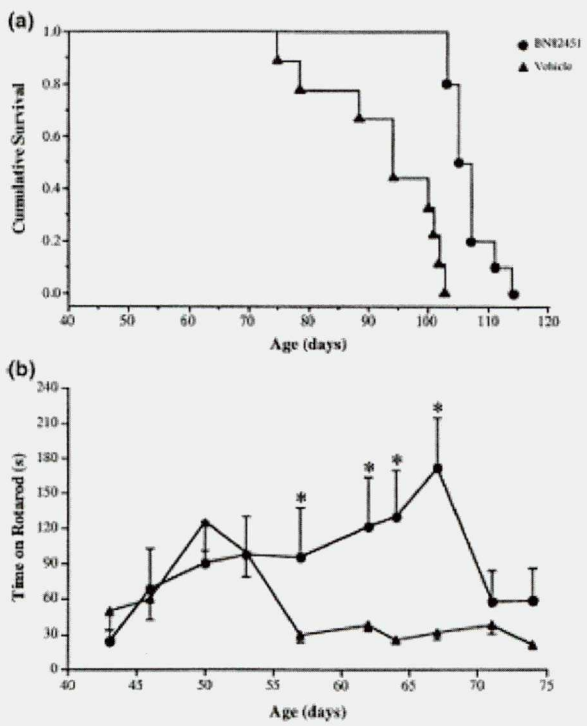

Figure 1

(a) Cumulative effect of BN82451 on survival in R6/2 transgenic mice; $p<0.001$ as compared with the controls.

(b) Effects of BN82451 on rotarod performance in R6/2 transgenic mice. The treatment significantly improved the motor performance on days 57, 60, 64 and 67 (*$p < 0.05$).

This compound did not delay the weight loss, as there were no differences in body weight between the groups (data not shown).

Oral administration of BN82451 attenuated the development of gross brain atrophy and ventricular enlargement at 10 weeks of age. At 70 days, the striatal volumes were as follows: BN82451-treated R6/2 mice: 702±41 mm^3; unsupplemented R6/2 mice: 576±63 mm^3, $p<0.01$.

The oral administration of BN82451 also attenuated the development of neuronal atrophy (Figure 2). Measured striatal neuron areas at 70 days: wild-type littermate control: 114±9.7 μm^2; BN82451-treated R6/2 mice: 79.5±11.1 μm^2; unsupplemented R6/2 mice: 48.1±17.2 μm^2; $p<0.01$. Lastly, the administration of BN82451 significantly attenuated the number of striatal ubiquitin-positive inclusions (Figure 3).

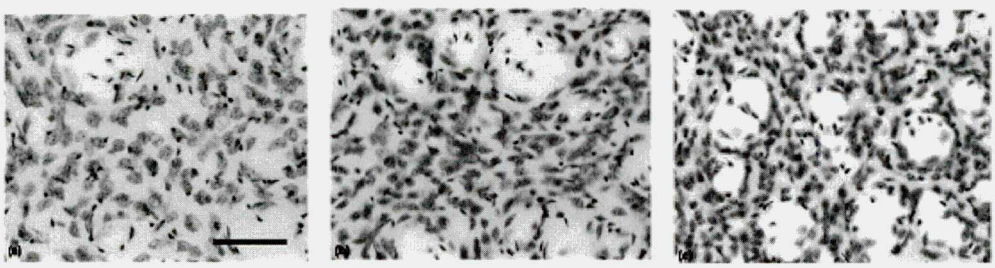

Figure 2
Nissl-stained tissue sections from the dorso-medial aspect of the neostriatum at the level of the anterior commissure in a littermate wild-type control mouse (a) a BN82451-treated R6/2 mouse (b) and an untreated R6/2 mouse (c) at 70 days of age. There is marked neuronal atrophy in the untreated R6/2 mouse, with relative preservation of the neuronal size in the BN82451-treated mouse, in comparison with the littermate control. Scale bar (shown in a): 100 μm.

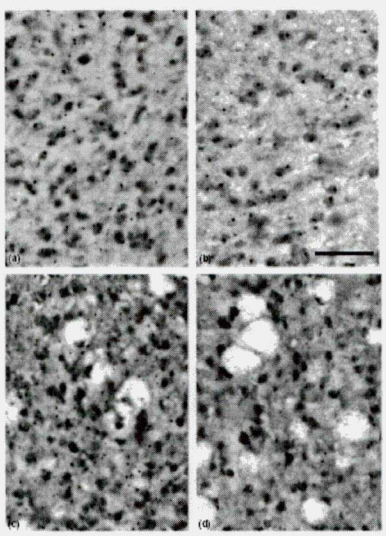

Figure 3
Ubiquitin-immunostained tissue sections from the neocortex (a and b) and neostriatum (c and d) of untreated (a and c) and BN82451-treated (b and d) R6/2 mice at 10 weeks of age. While there were reduced numbers of ubiquitin-positive inclusions in both the neocortex and the neostriatum of BN82451-treated mice, the difference was significant only in the neostriatum. Scale bar (shown in b): 100 μm.

IV.2. Sodium phenylbutyrate experiment – N171-82Q model

Systemic administration of sodium phenylbutyrate at a dose of 100 mg/kg ip, 6 days per week, starting at 75 days of age, produced a significant increase in survival of 23% in the N171-82Q transgenic mouse model of HD (Figure 4) ($p<0.0001$). The life span was 153.2±4.8 days in the sodium phenylbutyrate-treated mice and 124.5±5.4 days in the mice that received the vehicle. Surprisingly, sodium phenylbutyrate treatment did not have a significant effect on the weight loss or the motor performance, as assessed by rotarod performance in the N171-82Q mice (data not shown). The lack of beneficial effects on motor symptoms in the present study may reflect the fact that therapy was initiated after symptom onset.

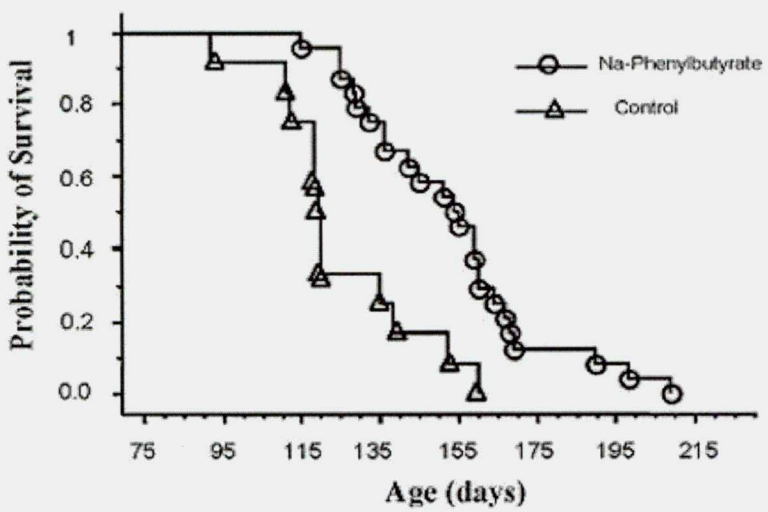

Figure 4
Effects of administration of sodium phenylbutyrate starting at 75 days of age on survival in the N171-82Q transgenic mouse model of HD. Sodium phenylbutyrate significantly improved the survival. (*$p<0.0001$,* Mantel-Cox log-rank test)

Histopathologic studies in brains of treated and untreated mice were performed at both 100 and 120 days of age. These studies revealed a significant attenuation of gross brain atrophy, ventricular hypertrophy and neuronal atrophy after sodium phenylbutyrate treatment, which was significant at 120 days (Figure 5). At 120 days, the total brain volume in the sodium phenylbutyrate-treated mice was 21.6% greater than for PBS ($p<0.01$), and the ventricular volume was 82.4% less ($p<0.001$). While marked striatal neuron atrophy was present in untreated N171-82Q mice at 120 days, sodium phenylbutyrate treatment significantly reduced the striatal neuron atrophy in N171-82Q mice (Wild-type littermate

control: 143.9±11.9 μm^2; sodium phenylbutyrate-treated N171-82Q mice: 116.5±17.5 μm^2; PBS-treated N171-82Q mice: 54.2±25.3 μm^2; sodium phenylbutyrate vs. PBS, $p<0.01$). The numbers of huntingtin and ubiquitin-stained aggregates were not altered by sodium phenylbutyrate administration. These results are similar to observations with sodium butyrate in the R6/2 transgenic mouse model of HD (Ferrante et al., 2003). Treatment with SAHA had no effect on the numbers of aggregates or the gross morphology, but there was a tendency to a reduction of neuronal atrophy (Hockly et al., 2003).

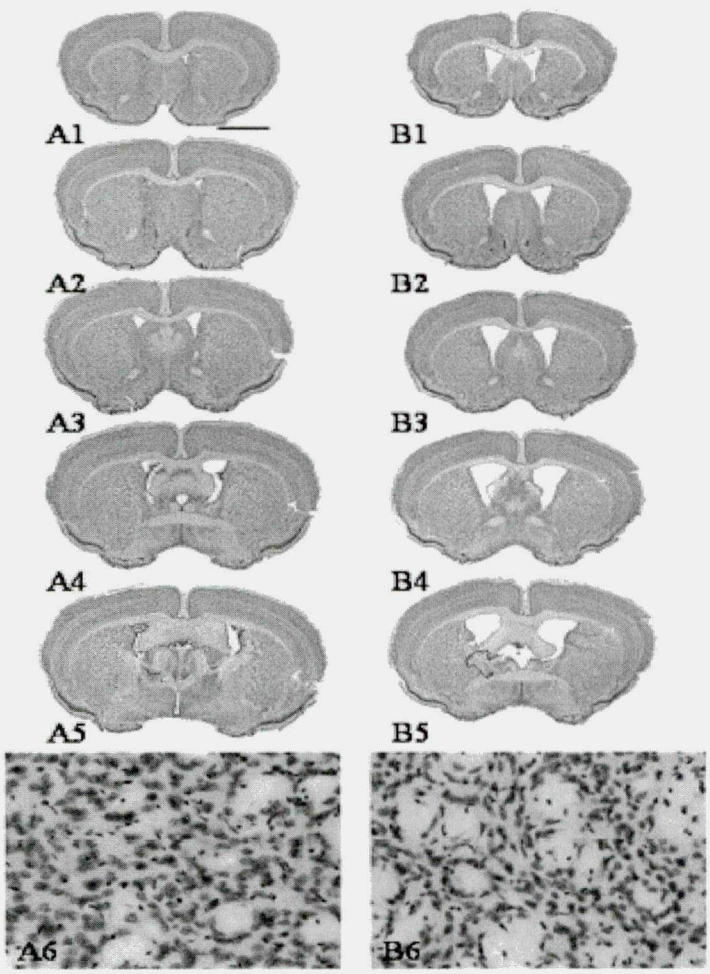

Figure 5
Gross brain and histopathological neuroprotection on sodium phenylbutyrate treatment.
Photomicrographs of coronal serial sections through the rostral neostriatum at the level of the anterior commissure in sodium phenylbutyrate-treated (A1-5) and PBS-treated (B1-5) N171-82Q HD transgenic mice at 120 days. There was gross atrophy of the brain in the PBS-treated N171-82Q mice together with ventricular hypertrophy. In contrast, the sodium phenylbutyrate-treated N171-82Q mice at 120 days (A) demonstrated significantly less atrophy and ventricular enlargement than the PBS-treated N171-82Q mice. Corresponding Nissl-stained tissue sections from the dorso-medial aspect of the neostriatum in sodium phenylbutyrate-treated (A6) and PBS-treated mice (B6) indicated marked neuronal atrophy in the PBS-treated N171-82Q mice. Scale bars in A and B indicate 2 mm except in A6 and B6, where it is 100 μm.

IV.3. Sodium phenylbutyrate experiment – N171-82Q model, gene expression

To verify that the effects we observed were due to an increase in histone acetylation, we performed both immunocytochemistry and Western blots. Administration of sodium phenylbutyrate for 2 weeks increased immunostaining for both acetylated H3 and H4 in striatal neurons (Figure 6).

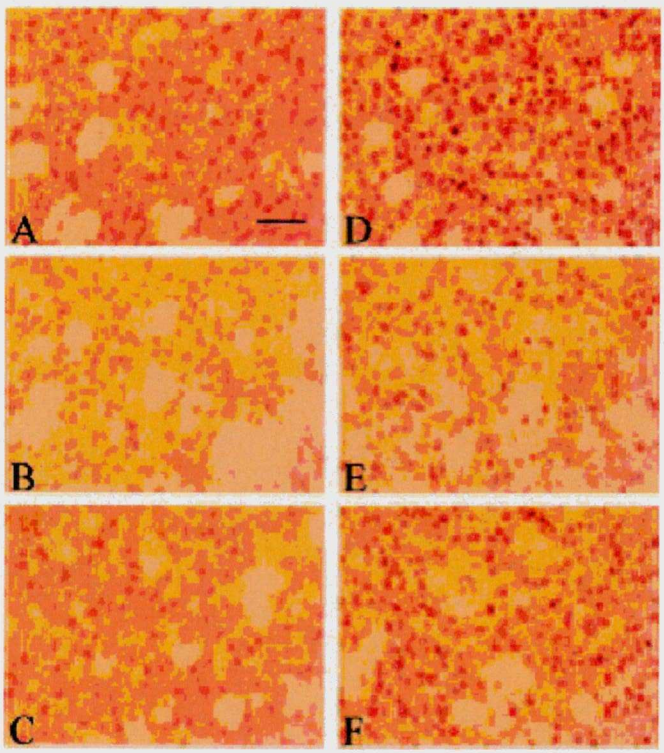

Figure 6
Striatal tissue immunohistochemistry of acetylated H3 (A, B, C) and H4 (D, E, F) in sodium phenylbutyrate-treated N171-82Q mice. Robust acetylated H3 and H4 immunohistochemistry was present in wild-type littermate control striatal tissue specimens (A and D, respectively), with hypoacetylation in the N171-82Q mice (B and E, respectively). Sodium phenylbutyrate treatment increased the acetylation of H3 and H4 in N171-82Q mice (C and F, respectively). The bar in A denotes 100 μm and applies to all Figures.

Administration of sodium phenylbutyrate at a dose of 100 mg/kg increased histone acetylation in the spleen (not shown) and brain at 2 h post-administration (Figure 7).

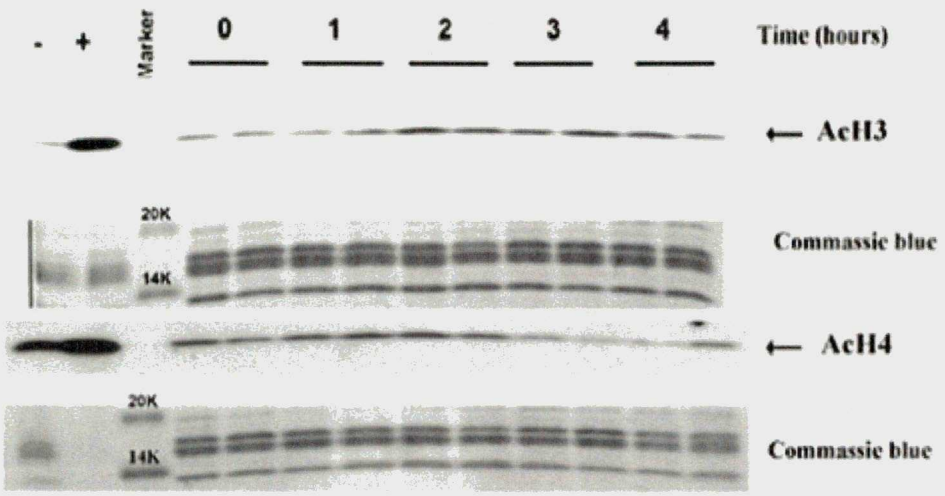

Figure 7
Western blots showing the effects of sodium phenylbutyrate treatment (100 mg/kg ip) on histone acetylation in the brain of N171-82Q mice at 0, 1, 2, 3 and 4 h after administration.
There were significant increases in acetylated H3 (AcH3) and H4 (AcH4) at 2 h ($p<0.05$ ANOVA followed by Newman-Keuls). Control histones from untreated (-) or sodium butyrate-treated (+) HeLa cells were used as a positive control for histone acetylation detection (lanes - and +, respectively).

Another histone modification which can repress gene transcription is methylation of lysine 9 on H3. Through immunocytochemistry, we found a marked increase in the methylation of H3 in the striatum at 120 days of age, which was markedly attenuated by sodium phenyl-butyrate treatment (Figure 8). This finding was confirmed by Western blotting (data not shown).

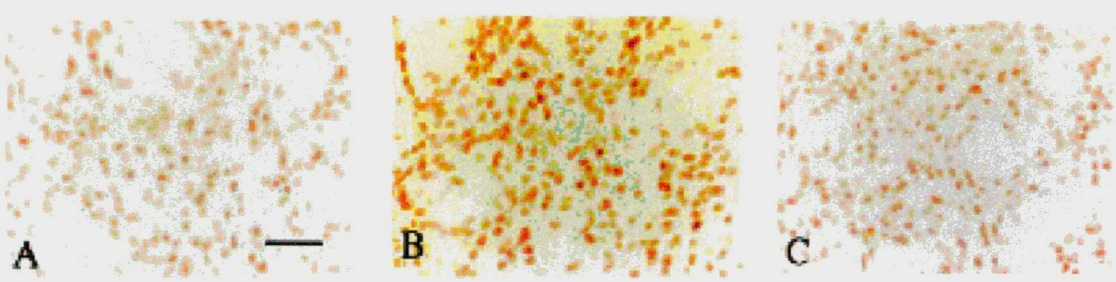

Figure 8
Striatal tissue immunohistochemistry for methylation of lysine 9 in H3 at 120 days of age.
The immunocytochemical staining for methylation is markedly increased in the N171-82Q mice (*B*) as compared with the wild-type controls (*A*). Sodium phenylbutyrate markedly attenuated the increase in methylation *(C)*. The bar in *A* indicates 100 μm and applies to all Figures.

We also examined the effects of sodium phenylbutyrate on the gene expression levels by using Affymetrix gene arrays. Sodium phenylbutyrate was administered for 2 weeks, starting at 75 days of age, to 5 N171-82Q mice, while 5 mice received the vehicle. The transcription products in the striatum of the two groups were compared. To validate the alterations in gene expression at the mRNA level, which appeared on the microarray, real-time PCR (RT-PCR) was performed with a LightCycler thermal cycler system. The expressions of selected genes (Gfer, Gstm3 and Psma3) were significantly upregulated after sodium phenylbutyrate treatment as compared with the controls ($p<0.05$), while other genes (Casp9, Cflar and Prkce) exhibited a significantly lower expression after sodium phenylbutyrate treatment than in the controls ($p<0.05$) (Figure 9). Since caspase 9 is involved in the activation of caspase 3, and is increased in HD patients, we examined the caspase 3 immuno-activity at 120 days of age. It was markedly increased in the striatum of the N171-82Q mice as compared with the controls, similarly as observed in the R6/2 mice. The increase was markedly attenuated by sodium phenylbutyrate treatment (data not shown).

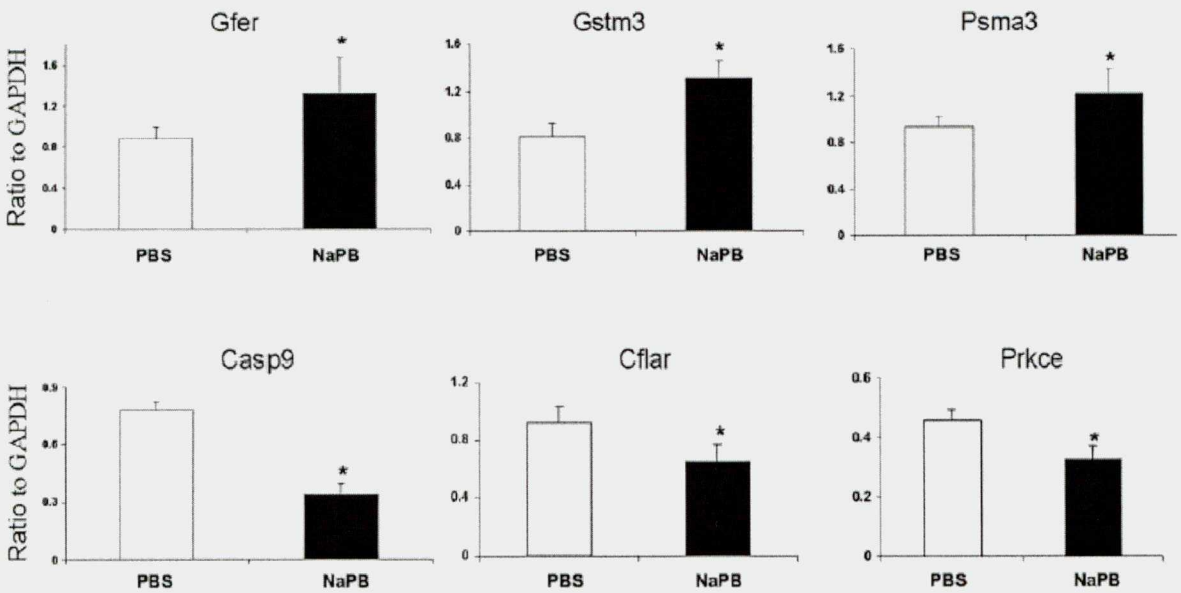

Figure 9
Quantitative real-time-PCR analysis of genes identified by microarray analysis as differentially expressed. Total RNA was extracted and real-time RT-PCR was performed with SYBR Green I dye, using a LightCycler thermal cycler system. The expression level is shown as the weight ratio of the target gene to GAPDH; Gfer (growth factor), Gstm3 (glutathione-S-transferase), Psma3 (proteasome subunit, α type 3), Casp9 (caspase 9), Cflar (CASP8 and Fas-activated death domain-like apoptosis regulator), and Prkce (protein kinase C). Data are means ± SEM for 4–5 samples, calculated by the comparative cycle threshold method. *$p<0.05$, as compared with PBS-injected mice

IV.4. Sodium phenylbutyrate experiment – MPTP model

As shown in Figure 10, MPTP administration produced significant reductions in dopamine, DOPAC and HVA. Administration of sodium phenylbutyrate starting 1 day before MPTP administration and then continuing until sacrifice 7 days later, produced significant protection against the depletion of dopamine, DOPAC and HVA.

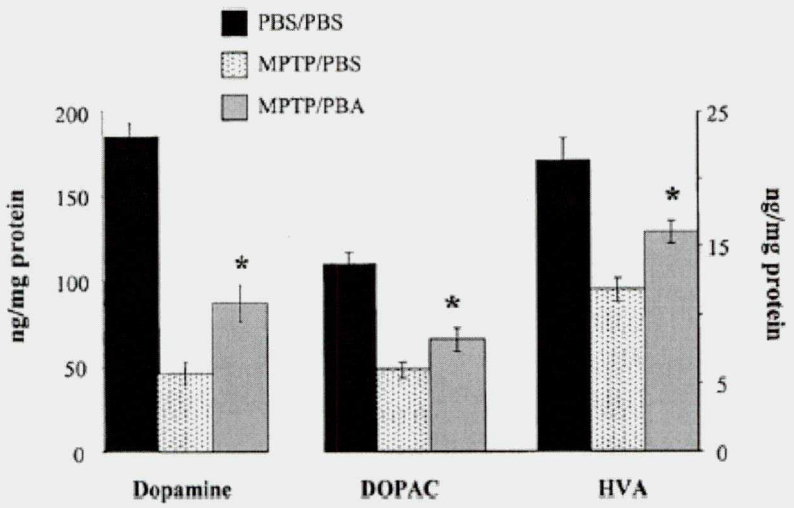

Figure 10
Effects of sodium phenylbutyrate on MPTP-induced depletion of dopamine and its metabolites DOPAC and HVA in the mouse striatum. $*p < 0.05$ as compared with MPTP alone.

MPTP significantly diminished the numbers of TH-immunoreactive neurons in the SNpc relative to the controls, by almost 50% ($p<0.001$) (Figures 11 and 12). Sodium phenylbutyrate treatment significantly attenuated the MPTP-induced decrease in the number of TH-positive neurons ($p<0.05$). The actual numbers of TH-positive neurons were 10420 ± 591 in the PBS controls, 5164 ± 559 in the MPTP-treated mice, and 7048 ± 643 in the MPTP + sodium phenylbutyrate-treated mice (Figures 11 and 12).

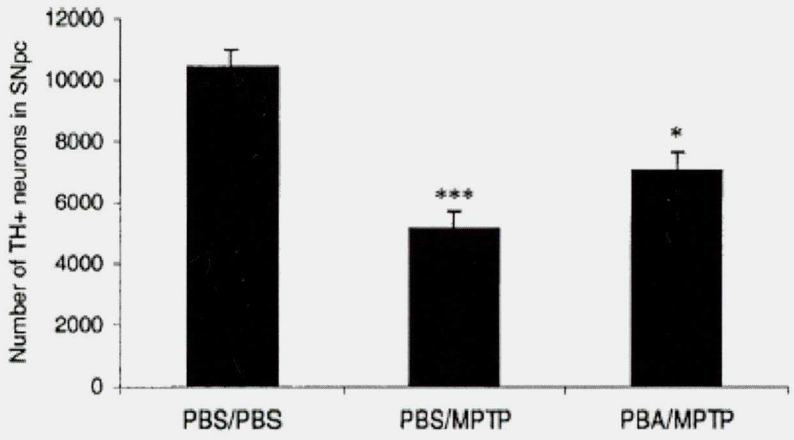

Figure 11
Effects of sodium phenylbutyrate (PBA) on MPTP-induced reduction of TH-immunoreactive neuron count in the SNpc. Stereological cell counts were made by using the optical fractionator method. Data are expressed as means ± SEM (PBS/PBS n = 5; PBS/MPTP n = 9; PBA/MPTP n = 9). *p < 0.05 vs PBS/MPTP, ***p < 0.001 vs PBS/PBS.

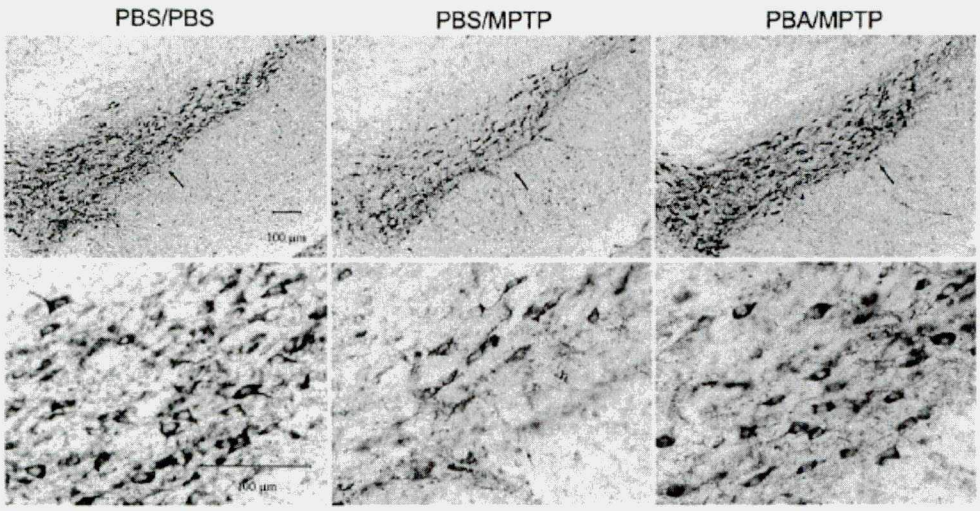

Figure 12
The immunoreactivity in representative sections through the substantia nigra control (PBS/PBS), MPTP-treated (PBS/MPTP), and MPTP + sodium phenylbutyrate-treated (PBA/MPTP) mice. Low- (top) and high- (bottom) magnification photomicrographs show MPTP-induced dopaminergic neuronal loss and its attenuation by sodium phenylbutyrate. Arrows indicate the respective areas magnified below.

V. DISCUSSION

V.1. BN82451 experiment – R6/2 model

Evidence is accumulating to suggest that certain chronic neurodegenerative disorders are caused by a combination of events that impair the normal neuronal function. Both excitotoxicity and oxidative damage contribute to the disease pathogenesis (Beal, 1995). Transgenic mice with full-length huntingtin expressed in a YAC construct display increased vulnerability to striatal excitotoxic lesions (Zeron et al., 2001, 2002). A secondary consequence of the excitotoxicity is oxidative damage (Beal, 1995). The expression of mutant huntingtin in neuronal and non-neuronal cells causes increased levels of reactive oxygen species, which contributes to cell death (Wyttenbach et al., 2002). A number of studies have demonstrated that there is increased oxidative damage in the R6/2 transgenic mouse model of HD. These mice display increased immunostaining for 3-nitrotyrosine, a marker of peroxynitrite-mediated oxidative damage (Tabrizi et al., 2000), together with increased and progressive lipid peroxidation (Perez-Severiano et al., 2000) in the brain and increased concentrations of a marker of oxidative damage to the DNA, 8-hydroxy-2-deoxyguanosine, in the urine, plasma and striatal microdialysates (Bogdanov et al., 2001). There is also evidence that inflammation may contribute to disease pathogenesis in R6/2 mice. Gene array studies reveal that there is an increased expression of genes associated with inflammation at both 6 and 12 weeks of age in R6/2 transgenic HD model (Luthi-Carter et al., 2000). There are also increased levels of interleukin-1b, a pro-inflammatory cytokine (Ona et al., 1999; Singhrao et al, 1999). Inhibition of the interleukin-1b converting enzyme by crossing transgenic mice with a dominant-negative inhibitor of this enzyme into R6/2 mice significantly extends the survival (Ona et al., 1999).

The present study therefore related to the effects of a novel compound, an orally active brain permeable antioxidant that not only acts as an inhibitor of lipid peroxidation, but which also has potent anti-inflammatory effects (Chabrier et al., 2001). BN82451 has previously been shown to exert neuroprotective effects in animal models in which a mitochondrial impairment was produced through the use of malonate or MPTP (Chabrier et al., 2001).

The present experiments indicated that BN82451 produced significant improvements in survival and rotarod performance in the R6/2 transgenic mouse model of HD. Surprisingly, there was no effect on the loss of body weight, suggesting that a delay of weight loss does not necessarily accompany improved survival. It also significantly reduced the striatal atrophy, the neuronal atrophy and the numbers of neuronal intranuclear inclusions. The 15.3% improvement in survival is equivalent to the effects of co-enzyme Q10 and minocycline, although slightly less than those of creatine and cystamine (Chen et al., 2000; Ferrante et al., 2000; Dedeoglu et al., 2002; Ferrante et al., 2002). Hence, these findings provide further evidence that both oxidative damage and inflammation may contribute to the disease pathogenesis. They raise the possibility that agents which have anti-oxidative and anti-inflammatory activity may be useful as therapies to slow or halt the progression of neurodegeneration in HD. These agents might also be useful in combination with others, such as creatine, co-enzyme Q10, minocycline and HDAC inhibitors in producing additive therapeutic benefits for the treatment of HD.

V.2. Sodium phenylbutyrate experiment – N171-82Q model

There is substantial evidence that an impaired gene transcription plays a role in the pathogenesis of HD. It has been demonstrated that huntingtin can bind directly to a number of transcription factors. These include the CREB binding protein (CBP), Sp1 and several others. The overexpression of either CBP or Sp1 can rescue cultured cells from the neurotoxicity of mutant huntingtin (Nucifora et al., 2001, Dunah et al., 2002). Earlier studies had shown that treatment with HDAC inhibitors is effective in attenuating polyglutamine toxicity *in vitro* (Hughes et al., 2001; McCampbell et al., 2001). Treatment with HDAC inhibitors arrests on-going progressive neuronal degeneration in a *Drosophila* model of polyglutamine neurotoxi-city (Steffan et al., 2001). The HDAC inhibitor SAHA improves the motor function (Hockly et al., 2003), and sodium butyrate improves the motor function and exerts neuroprotective effects when administered presymptomatically in the R6/2 model of HD (Ferrante et al., 2003).

In the present study, the HDAC inhibitor sodium phenylbutyrate was administered to the N171- 82Q transgenic mouse model of HD. The administration of sodium phenylbutyrate from 75 days of age was found to produce a significant (23%) improvement in survival. This is particularly impressive because the start-point of therapy, at 75 days, is a timepoint after

which the N171-82Q mice exhibit initial symptoms (Schilling et al., 1999, 2001). The findings are robust and the 23% increase in survival is the best overall therapeutic effect yet reported in the N171-82Q HD model. Other therapies are much less effective when initiated after onset of the symptoms. Administration of a combination of coenzyme Q10 and remacemide to N171-82Q mice from 21 days of age extended the survival by 17% and improved the motor performance (Ferrante et al., 2002), though when this dosing regimen was initiated at 56 days of age, the motor performance deterioration was delayed, but there was no beneficial effect on survival (Schilling et al., 2001). The finding that sodium phenylbutyrate is effective in symptomatic transgenic HD mice is consistent with the observations on a *Drosophila* model of polyglutamine toxicity that HDAC inhibitors are neuroprotective even when administered to animals already exhibiting neurodegeneration (Steffan et al., 2001). Moreover, sodium phenylbutyrate extends the lifespan in wild-type *Drosophila* when administered late in life (Kang et al., 2002).

Surprisingly, there was no significant effect on the weight loss or motor deficits, which may reflect the fact that the therapy was initiated after symptom onset. Similarly, SAHA did not affect the weight loss, although it improved both the rotarod performance and the grip strength when administered presymptomatically (Hockly et al., 2003).

Histopathologic studies on the action of sodium phenylbutyrate in N171-82Q mice demonstrated a trend toward reduced atrophy at 100 days of age. At 120 days of age, there were significant reductions in gross brain atrophy, ventricular enlargement and striatal neuron atrophy. Presymptomatic treatment with sodium butyrate also attenuates brain atrophy, ventricular enlargement and striatal neuron atrophy (Ferrante et al., 2003). Interestingly, sodium phenylbutyrate treatment had no effect on huntingtin and ubiquitin-stained aggregates, which is consistent with observations relating to SAHA and sodium butyrate (Ferrante et al., 2003; Hockly et al., 2003). The effects of HDAC inhibitors contrast with the therapeutic effects of agents such as creatine, coenzyme Q10 with remacemide and cystamine, which significantly reduce the number of huntingtin immunoreactive aggregates (Huntington Study Group, 2001; Andreassen et al., 2001; Dedeoglu et al., 2002, 2003; Ferrante et al., 2002). Minocycline and dichloroacetate also increase the survival in transgenic HD mice, without altering the aggregate load (Chen et al., 2000; Andreassen et al., 2001). Our findings therefore

provide further evidence that therapeutic effects in transgenic mouse models of HD can occur independently of effects on aggregate deposition.

V.3. Sodium phenylbutyrate experiment – N171-82Q model, gene expression

We verified that sodium phenylbutyrate increases the acetylation of both H3 and H4 in the brains of treated mice, using both immunocytochemistry and Western blotting. We also examined histone methylation. While histone acetylation is thought to relax the chromatic structure leading to increased gene transcription, subsequent histone methylation (particularly on lysine 9 of H3) leads to transcriptional repression, assisting the termination of gene transcription (Zhang et al., 2001). Prior studies revealed interactions between HDACs and histone methyltransferases that repress transcription (Pal et al., 2003; Gui et al., 2004). DNA methyltransferases which repress transcription also interact with HDACs (Deplus et al., 2002; Sekimata et al., 2001). We have observed for the first time a marked increase in the methylation of lysine 9 of H3 in symptomatic N171-82Q mice relative to the wild-type level, which was markedly attenuated by treatment with sodium phenylbutyrate. This finding suggests that sodium phenylbutyrate mediates its effects both by increasing histone acetylation and by reducing histone methylation, thereby increasing the expression of genes critical to cell survival.

We also examined the effects of sodium phenylbutyrate on gene expression levels. Genes which displayed significant increases in expression following sodium phenylbutyrate administration included glutathione-S-transferase, striatin calmodulin-binding protein 3, ubiquitin specific protease 29, proteosome subunit alpha type 3 and the proteosome 26S subunit (ATPase 3), whereas caspase 9, caspase 8/FADD-like apoptosis regulator and proteasome 26S subunit (non-ATPase 10) were significantly decreased. Consistent with the upregulation of caspase 9, active caspase 3 was also increased in the striatum, and this increase was attenuated by sodium phenylbutyrate treatment. Since aberrant protein degradation and apoptosis are implicated in HD pathogenesis, these alterations may contribute to the therapeutic effects of sodium phenylbutyrate (Jana et al., 2001; Friedlander, 2003).

Our findings show that administration of the HDAC inhibitor sodium phenylbutyrate exerts neuroprotective effects and increases the survival in symptomatic HD transgenic mice, supporting studies in which HDAC inhibitors were administered presymptomatically (Ferrante

et al., 2003; Hockly et al., 2003). Sodium phenylbutyrate is a particularly promising agent for therapeutic trials in man: extensive experience is available concerning its use in patients for the treatment of urea cycle disorders, sickle cell anemia, thalassemia minor, and cystic fibrosis (Dover et al., 1994; Rubenstein et al., 1998; Hoppe et al., 1999). Patients with ornithine transcarbamylase deficiency have been treated long-term with doses of sodium phenylbutyrate in the range 350-600 mg/kg/day without significant side-effects (Maestri et al., 1996; Burlina et al., 2001). Phase one trials in cancer patients showed good tolerability at doses of 400-500 mg/kg/day (Carducci et al., 2001; Gilbert et al., 2001). Our effective dose of 100 mg/kg/day in mice is therefore well within the tolerable range. These findings suggest that sodium phenylbutyrate is an extremely promising agent for the treatment of HD.

V.4. Sodium phenylbutyrate experiment – MPTP model

We examined the ability of the HDAC inhibitor sodium phenylbutyrate to exert neuroprotective effects against lesions produced by the mitochondrial toxin MPTP. MPTP neurotoxicity is thought to be mediated by a mitochondrial dysfunction and oxidative damage.
Feeding sodium phenylbutyrate to *Drosophila* markedly increases its life span, and this is accompanied by a large increase in the expression of manganese superoxide dismutase (Kang et al., 2002). The expression of a number of other antioxidant enzymes, e.g. glutathione-S-transferase, and chaperone proteins, e.g. heat shock protein 70, were also increased. The administration of HDAC inhibitors can lead to the acetylation of Sp1, which has been implicated in resistance to oxidative stress (Ryu et al., 2003). HDAC inhibitors also inhibit inflammation by suppressing cytokines. The administration of SAHA to mice dose-dependently reduced the lipopolysacchride-induced increases in plasma tumor necrosis factor-α, interleukin-1β, interleukin-6, and interferon-γ (Leoni et al., 2002).

In the present study, we found that sodium phenylbutyrate administration exerted significant neuroprotective effects against the MPTP-induced depletion of striatal dopamine lesions, and also the loss of TH-immunoreactive neurons in the substantia nigra. The mechanism of the neuroprotective effects could involve either the improved mitochondrial function or the induction of antioxidative enzymes and protein chaperones. These results suggest that HDAC inhibitors have the potential to exert neuroprotective effects in PD.

VI. CONCLUSIONS

1. BN82451, which has antioxidant effects and anti-inflammatory activities, blocks microglial activation and inhibits cyclooxygenases, produced significant improvements in survival and rotarod performance in the R6/2 transgenic mouse model of HD.
2. Administration of the HDAC inhibitor sodium phenylbutyrate exerts neuroprotective effects and increases the survival in symptomatic HD transgenic mice. Our findings indicate that sodium phenylbutyrate mediates its effects both by increasing histone acetylation and reducing histone methylation, thereby increasing the expressions of genes critical to cell survival. These observations suggest that sodium phenylbutyrate administration may be beneficial to HD patients after the onset of symptoms.
3. Sodium phenylbutyrate exerts neuroprotective effects against lesions produced by the mitochondrial toxin MPTP.

The pathogenesis of neuronal degeneration in HD and PD is an area of intense investigation. Evidence is accumulating to suggest that such chronic neurodegenerative disorders are caused by a combination of events that impair the normal neuronal function. Excitotoxicity, oxidative damage, inflammation, altered gene expression and protein misfolding contribute to the disease pathogenesis. Sodium phenylbutyrate is a particularly promising agent for therapeutic trials in man in consequence of the extensive experience available on its use in patients for the treatment of, for example, cancer, hemoglobinopathy and cystic fibrosis. It is also possible that BN82451 might be useful in combination with other agents such as creatine, co-enzyme Q10, minocycline and HDAC inhibitors in producing additive therapeutic benefits for the treatment of HD and PD.

There are currently no cures or even effective therapies for HD. However, recent advances in understanding have provided new hope that a therapeutic strategy might one day be possible.

ACKNOWLEDGMENTS

I would like to express my gratitude to Professor László Vécsei, Member of the Hungarian Academy of Sciences, Director of the Department of Neurology, University of Szeged, who made my work possible and for his scientific guidance. I am deeply indebted to Professor M. Flint Beal at Cornell University, New York, USA, not only for his excellent scientific advice and encouragement, but for the opportunity to work in his laboratory, where the animal experiments were performed.

I wish to thank all my co-workers with whom I performed the experiments: Péter Klivényi, M.D., Ph.D. (Department of Neurology, University of Szeged), Jason Gregorio, Noel Y Calingasam, Lichuan Yang M.D., Dong-Kug Choi M.D., Ph.D., Linda Metakis (Cornell University, USA) and Katalin Jakab M.D., Ph.D. (Department of Neurology, University of Szeged)

Last, but not least, I thank my family and friends for their endless support during my work.

REFERENCES

1. Andreassen OA, Dedeoglu A, Ferrante RJ, Jenkins BG, Ferrante KL, Thomas M, Friedlich A, Browne SE, Schilling G, Borchelt DR, Hersch SM, Ross CA, Beal MF (2001) Creatine increases survival and delays motor symptoms in a transgenic animal model of Huntington's disease. *Neurobiol Dis* 8:479-491.
2. Andreassen OA, Ferrante RJ, Huang HM, Dedeoglu A, Park L, Ferrante KL, Kwon J, Borchelt DR, Ross CA, Gibson GE, and Beal MF (2001) Dichloroacetate exerts therapeutic effects in transgenic mouse models of Huntington's disease. *Ann Neurol* 50, 112–117.
3. Ausubel FM, Brent R, Kingston RE, Moore DD, Seidman JG, Smith JA, Struhl K (eds.) (2000) *Current protocols in molecular biology*. pp:61-111, Wiley, New York.
4. Petersen A, Mani K, Brundin P (1999) Recent advances on the pathogenesis of Huntington's disease. *Exp Neurology* 157:1-18.
5. Bates GP, Mangiarini L, Mahal A, Davies SW (1997) Transgenic models of Huntington's disease. *Hum Mol Genet* 10:1633-1637.
6. Bates GP (2001) Huntington's disease. Exploiting expression. Nature 413:691, 693-694.
7. Beal MF, Kowall NW, Ellison DW, Mazurek MF, Swartz KJ, Martin JB (1986) Replication of the neurochemical characteristics of Huntington's disease by quinolinic acid. *Nature* 321:168-171.
8. Beal MF, Matson WR, Swartz KJ, Gamache PH, and Bird ED (1990) Kynurenine pathway measurements in Huntington's disease striatum: evidence for reduced formation of kynurenic acid. *J Neurochem* 55:1327–1339.
9. Beal MF (1992) Does impairment of energy metabolism result in excitotoxic neuronal death in neurodegenerative illnesses? *Ann Neurology* 31: 119-130.
10. Beal MF (1995) Effects of mitochondrial toxins in animals and man. In: Beal MF: Mitochondrial dysfunction and oxidative damage in neurodegenerative diseases. Springer-Verlag.
11. Beal MF (1995) Aging, energy and oxidative stress in neurodegenerative diseases. *Ann Neurol* 38:357-366.
12. Beal MF (1997) Oxidative damage in neurodegenerative diseases. *The Neuroscientist* 3: 21-27.
13. Beal MF (2001) Experimental models of Parkinson's disease. *Nature Reviews* 2:326-332.

14. Bogdanov MB, Andreassen OA, Dedeoglu A, Ferrante RJ, and Beal MF (2001) Increased oxidative damage to DNA in a transgenic mouse model of Huntington's disease. *J Neurochem* 79:1246–1249.

15. Burlina AB, Ogier H, Korall H, and Trefz FK (2001) Long-term treatment with sodium phenylbutyrate in ornithine transcarbamylase-deficient patients. *Mol Genet Metab* 72:351–355.

16. Carducci MA, Gilbert J, Bowling MK, Noe D, Eisenberger MA, Sinibaldi V, Zabelina Y, Chen TL, Grochow LB, and Donehower RC (2001) A Phase I clinical and pharmacological evaluation of sodium phenylbutyrate on an 120-h infusion schedule. *Clin Cancer Res* 7:3047–3055.

17. Cepade C, Ariano MA, Calvert CR, Flores-Hernandez J, Chandler SH, Leavitt BR, Hayden MR, Levine MS (2001) NMDA receptor function in mouse models of Huntington's disease. *J Neurosci Res* 66:525-539.

18. Chabrier PE, Roubert V, Harnett J, Cornet S, Delafotte S, Charnet-Roussillot C, Spinnewyn B and Auguet M (2001) New neuroprotective agents are potent inhibitors of mitochondrial toxins: in vivo and in vitro studies. *Soc Neurosci Abstr.* 27: 530.

19. Chang KT, Min KT (2002) Regulation of lifespan by histone deacetylase. *Aging Research Reviews* 313-326.

20. Chen M, Ona VO, Li M, Ferrante RJ, Fink KB, Zhu S, Bian J, Guo L, Farrell LA, Hersch SM, Hobbs W, Vonsattel JP, Cha JH, Friedlander RM (2000) Minocycline inhibits caspase-1 and caspase-3 expression and delays mortality in a transgenic mouse model of Huntington disease. *Nat Med* 6: 797-801

21. Coyle JF, Schwarcz R (1976) Leison of striatal neurons with kainic acid provides a model of Huntington's chorea. *Nature* 263:244-246.

22. Csillik A, Knyihar E, Okuno E, Krisztin-Peva B, Csillik B, Vecsei L (2002) Effect of 3-Nitropropionic Acid on kynurenine aminotransferase in the rat brain. *Exp Neurol* 177:233-241.

23. Dedeoglu A, Jeitner TM, Matson SA, Kubilus JK, Bogdanov M, Kowall NW, Matson WR, Cooper AL., Ratan RR, Beal MF, Hersch SM and Ferrante RJ (2002) Therapeutic effects of the transglutaminase inhibitor, cystamine, in a murine model of Huntington's disease. *J Neurosci* 22: 8942–8950.

24. Dedeoglu A, Kubilus JK, Yang L, Ferrante KL, Hersch SM, Beal MF, and Ferrante RJ (2003) Creatine therapy provides neuroprotection after onset of clinical symptoms in Huntington's disease transgenic mice. *J Neurochem* 85:1359–1367.

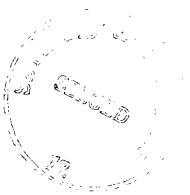

25. Deplus R, Brenner C, Burgers WA, Putmans P, Kouzarides T, de Launoit Y, and Fuks F (2002) Dnmt3L is a transcriptional repressor that recruits histone deacetylase. *Nucleic Acids Res* 30:3831–3838.

26. DiFiglia M (1990) Excitotoxic injury of the neostriatum: a model for Huntington's disease. *Trends in Neurosciences* 13:286-289.

27. DiFiglia M, Sapp E, Chase KO, Davies SW, Bates GP, Vonsattel JP, Aronin N (1997) Aggregation of huntingtin in neuronal intranuclear inclusions and dystrophic neuritis in brain. *Science* 277:1990-1993.

28. Di Prospero NA and Fischbeck KH (2005) Therapeutics development for triplet repeat expansion diseases. *Nat Rev Gen* 6:756-765.

29. Dover GJ, Brusilow S, and Charache S (1994) Induction of fetal hemoglobin production in subjects with sickle cell anemia by oral sodium phenylbutyrate. *Blood* 84:339–343.

30. Dunah AW, Jeong H, Griffin A, Kim YM, Standaert DG, Hersch SM, Mouradian MM, Young AB, Tanese N, and Krainc D (2002) Sp1 and TAFII130 transcriptional activity disrupted in early Huntington's disease. *Science* 296:2238–2243.

31. Ferrante RJ, Kowall NW, Beal MF, Richardson EP, Bird EB, Martin JB (1985) Selective sparing of a class of striatal neurons in Huntington's disease. *Science* 230: 561-563.

32. Ferrante RJ, Andreassen OA, Jenkins BG, Dedeoglu A, Kuemmerle S, Kubilus JK, Kaddurah-Daouk R, Hersch SM, Beal MF (2000) Neuroprotective effects of creatine in a transgenic mouse model of Huntington's disease. *J Neurosci* 20:4389-4397.

33. Ferrante RJ, Andreassen OA, Dedeoglu A, Ferrante KL, Jenkins BG, Hersch SM and Beal MF (2002) Therapeutic effects of coenzyme Q10 and remacemide in transgenic mouse models of Huntington's disease. *J Neurosci* 22: 1592–1599.

34. Ferrante RJ, Kubilus JK, Lee J, Ryu H, Beesen A, Zucker B, Smith K, Kowall NW, Ratan RR, Luthi-Carter R, Hersch SM (2003) Histone deacetylase inhibition by sodium butyrate chemotherapy ameliorates the neurodegenerative phenotype in Huntington's disease mice. *J Neurosci* 23:9418-9427.

35. Forno LS, Langston JW, DeLanney LE, Irwin I (1988) An electron microscopic study of MPTP-induced inclusion bodies in an old monkey. *Brain Res* 448:150-157.

36. Friedlander RM (2003) Apoptosis and caspases in neurodegenerative diseases. *N. Engl. J. Med.* 348:1365–1375.

37. Fu YH, Kuhl DP, Pizzuti A, Pieretti M, Sutcliffe JS, Richards S, Verkerk AJ, Holden JJ, Fenwick RG Jr, Warren ST (1991) Variation of the CGG repeat at the fragile X site results in genetic instability: resolution of the Sherman paradox. *Cell* 67:1047-1058.

38. Garron DC (1973) Behavioral aspects of Huntington's chorea. *Adv Neurol* 1:729-735.

39. Gilbert J, Baker SD, Bowling MK, Grochow L, Figg WD, Zabelina Y, Donehower RC, and Carducci MA (2001) A phase I dose escalation and bioavailability study of oral sodium phenylbutyrate in patients with refractory solid tumor malignancies. *Clin Cancer Res* 7:2292–2300.

40. Gui CY, Ngo L, Xu WS, Richon VM, and Marks PA (2004) Histone deacetylase (HDAC) inhibitor activation of p21WAF1 involves changes in promoter-associated proteins, including HDAC1. *Proc Natl Acad Sci USA* 101:1241–1246.

41. Gusella JF, MacDonald ME, Ambrose CM, Duyao MP (1993) Molecular genetics of Huntington's disease. *Arch Neurol* 50:1157-63.

42. Hague SM, Klaffke S, Bandmann O (2005) Neurodegenerative disorders: Parkinson's disease and Huntington's disease. *J Neurol Neurosurg Psychiatry* 76:1058-1063.

43. Harjes P and Wanker EE (2003) The hunt for huntingtin function: interaction partners tell many different stories. *Trends Biochem Sci* 28:425-433.

44. Hedreen JC, Peyser CE, Folstein SE, Ross CA (1991) Neuronal loss in layer V and VI of cerebral cortex in HD. *Neurosci Lett* 33:257-261.

45. Hockly E, Richon VM, Woddman B, Smith DL, Zhou X, Rosa E, Sathasivam K, Ghazi-Noori S, Mahal A, Lowden PA, Steffan JS, Marsh JL, Thompson LM, Lewis CM, Marks PA, Bates GP (2003) Subeorylanilide hydroxami acid, a histone deacetylase inhibitor, ameliorates motor deficits in a mouse model of Huntington's disease. *Proc Natl Acad Sci USA* 100:2041-2046.

46. Hoppe C, Vichinsky E, Lewis B, Foote D, and Styles L (1999) Hydroxyurea and sodium phenylbutyrate therapy in thalassemia intermedia. *Am J Hematol* 62:221–227.

47. Hoshino M, Tagawa K, Okuda T, Murata M, Oyanagi K, Arai N, Mizutani T, Kanazawa I, Wanker EE, Okazawa H (2003) Histone deacetylase is retained in primary neurons expressing mutant huntingtin protein. *J Neurochem* 87:257-267.

48. Huntington's Disease Collab Res Grp. (1993) A novel gene containing a trinucleotide repeat that is expanded and unstable on Huntington's disease chromosomes. *Cell* 72:971-983.

49. Huntington Study Group (2001) A randomized, placebo-controlled trial of co-enzyme Q10 and remacemide in Huntington's disease. *Neurology* 57:397-404.

50. Hughes RE, Lo RS, Davis C, Strand AD, Neal CL, Olson JM, and Fields S (2001) Altered transcription in yeast expressing expanded polyglutamine. *Proc Natl Acad Sci USA* 98:13201–13206.

51. Jana NR, Zemskov EA, Wang GH, and Nukina N (2001) Altered proteasomal function due to the expression of polyglutamine-expanded truncated N-terminal huntingtin induces apoptosis by caspase activation through mitochondrial cytochrome c release. *Hum Mol Genet* 10:1049–1059.

52. Jenkins BG, Andreassen OA, Dedeoglu A, Leavitt B, Hayden M, Borchelt D, Ross CA, Detloff P, Ferrante RJ, and Beal MF (2005) Effects of CAG repeat length, HTT protein length and protein context on cerebral metabolism measured using magnetic resonance spectroscopy in transgenic mouse models of Huntington's disease. *J Neurochem* 95:553-562.

53. Kang HL, Benzer S, and Min KT (2002) Life extension in Drosophila by feeding a drug. *Proc Natl Acad Sci USA* 99:838–843.

54. Kieburtz K, Feigin A, McDermott M, Como P, Abwender D, Zimmerman C, Hickey C, Orme C, Claude K, Sotack J, Greenamyre JT, Dunn C, Shoulson I (1996) A controlled trial of remacemide hydrocloride in Huntington's disease. *Mov Disord* 11:272-277.

55. Kiechle T, Dedeoglu A, Kubilus J, Kowall NW, Beal MF, Friedlander RM, Hersch SM, and Ferrante RJ (2002) Cytochrome C and caspase-9 expression in Huntington's disease. *Neuromol Med* 1:183–195.

56. Krämer OH, Göttlicher M, Heinzel T (2001) Histone deacetylase as a therapeutic target. *Trends End Met* 12: 294-300.

57. Kremer B, Goldberg P, Andrew SE, Theilmann J, Telenius H, Zeisler J, Squitieri F, Lin B, Basset A, Almqvist E, Bird TD, Hayden MR (1994) A worldwide study of the Huntington's disease mutation--The sensitivity and specificity of measuring CAG repeats. *N Engl J Med* 330:1401-1406.

58. Leoni F, Zaliani A, Bertolini G, Porro G, Pagani P, Pozzi P, Dona G, Fossati G, Sozzani S, Azam T, Bufler P, Fantuzzi G, Goncharov I, Kim SH, Pomerantz BJ, Reznikov LL, Siegmund B, Dinarello CA, Mascagni P (2002) The antitumor histone deacetylase inhibitor suberoylanilide hydroxamic acid exhibits antiinflammatory properties via suppression of cytokines. *Proc. Natl. Acad. Sci. USA* 99, 2995–3000

59. Li XJ, Li SH, Sharp AH, Nucifora FC, Schilling G, Lanahan A, Worley P, Snyder SH, Ross CA (1995) A huntingtin-associated protein enriched in brain with implications for pathology. *Nature* 378:398-402.

60. Ludolph AC, He F, Spencer PS (1991) 3-Nitropropionic acid – exogenous animal neurotoxin and possible human striatal toxin. *Can J Neurol Sci* 18:492-498.

61. Ludolph AC, Seeling M, Ludolph A (1992) 3-Nitropropionic acid decreases cellular energy levels and causes neuronal degeneration in cortical explants. *Neurodegeneration* 1:155-161.

62. Luthi-Carter R, Strand A, Peters NL, Solano SM, Hollingsworth ZR, Menon AS, Frey AS, Spector BS, Penney EB, Schilling G, Ross CA, Borchelt DR, Tapscott SJ, Young AB, Cha JH, Olson JM (2000) Decreased expression of striatal signaling genes in a mouse model of Huntington's disease. *Hum Mol Genet* 9:1259-1271.

63. Maestri NE, Brusilow SW, Clissold DB, and Bassett SS (1996) Long-term treatment of girls with ornithine transcarbamylase deficiency. *N Engl J Med* 335:855–859.

64. Manfredi G, Beal F (2000) The role of mitochondria in the pathogenesis of neuro-degenerative diseases. *Brain Pathology* 10:462-472.

65. Mangiarini L, Sathasivam K, Seller M, Cozens B, Harper A, Hetherington C, Lawton M, Trottier Y, Lehrach H, Davies SW, Bates GP (1996) Exon 1 of the HD gene with an expanded CAG repeat is sufficient to cause progressive neurological phenotype in transgenic mice. *Cell* 87:493-506.

66. Marks PA, Richon VM, Breslow R, Rifkind RA (2001) Histone deacetylase inhibitors as new cancer drugs. *Curr Opin Oncol* 13:477-483.

67. McCampbell A, Taye AA, Whitty L, Penney E, Steffan JS, Fischbeck KH (2001) Histone deacetylase inhibitors reduce polyglutamine toxicity. *Proc Natl Acad Sci* 98: 15179-15184.

68. McGeer EG, McGeer PL (1976) Duplication of biochemical changes of Huntington's chorea by intrastriatal injection of glutamic and kainic acids. *Nature* 263:517-519.

69. Nucifora FC Jr, Sasaki M, Peters MF, Huang H, Cooper JK, Yamada M, Takahashi H, Tsuji S, Troncoso J, Dawson VL, Dawson TM, and Ross CA (2001) Interference by huntingtin and atrophin-1 with CBP-mediated transcription leading to cellular toxicity. *Science* 291:2423–2428.

70. Olney JW (1969) Brain lesions, obesity, and other disturbances in mice treated with monosodium glutamate. *Science* 164:719-721.

71. Ona VO, Li M, Vonsattel JP, Andrews LJ, Khan SQ, Chung WM, Frey AS, Menon AS, Li XJ, Stieg PE, Yuan J, Penney JB, Young AB, Cha JH and Friedlander RM (1999) Inhibition of caspase-1 slows disease progression in a mouse model of Huntington's disease. *Nature* 399: 263–267.

72. Pal S, Yun R, Datta A, Lacomis L, Erdjument-Bromage H, Kumar J, Tempst P, and Sif S (2003) mSin3A/histone deacetylase 2- and PRMT5-containing Brg1 complex is involved in transcriptional repression of the Myc target gene cad. *Mol Cell Biol* 23:7475–7487.

73. Perez-Severiano F, Rios C and Segovia J (2000) Striatal oxidative damage parallels the expression of a neurological phenotype in mice transgenic for the mutation of Huntington's disease. *Brain Res* 862: 234–237.

74. Perutz MF, Johnson T, Suzuki M, Finch JT. (1994) Glutamine repeats as polar zippers: Their possible role in inherited neurodegenerative diseases. *Proc Natl Acad Sci USA* 91:5355-5358.

75. Reiner A, Albin RL, Anderson KD, D'Amato JD, Penney JB, Young AB 1988) Differential loss of striatal projection neurons in Huntington's disease. *Proc Natl Acad Sci USA* 85: 5733-5737.

76. Richon VM, Sandhoff TW, Rifkind RA, Marks PA (2000) Histone deacetylase inhibitor selectively induces p21WAF1 expression and gene-associated histone acetylation. *Proc Natl Acad Sci U.S.A.* 97:10014-10019.

77. Ryu H, Lee J, Olofsson BA, Mwidau A, Dedeoglu A, Escudero M, Flemington E, Azizkhan-Clifford J, Ferrante RJ, and Ratan RR (2003) Histone deacetylase inhibitors prevent oxidative neuronal death independent of expanded polyglutamine repeats via an Sp1-dependent pathway. *Proc Natl Acad Sci USA* 100:4281–4286.

78. Rubenstein RC and Zeitlin PL (1998) A pilot clinical trial of oral sodium 4-phenylbutyrate (Buphenyl) in deltaF508-homozygous cystic fibrosis patients: partial restoration of nasal epithelial CFTR function. *Am J Respir Crit Care Med* 157:484–490.

79. Rubinsztein DC, Leggo J, Coles R, Almqvist E, Biancalana V, Cassiman JJ, Chotai K, Connarty M, Cranford D, Curtis A, Davidson MJ, Differ AM, Dode C, Dodge A, Frontali M, Ramen NG, Stine OC, Sherr M, Abbott MH, Franz ML, Graham CA, Harper PS, Hedreen JC, Hayden MR (1996) Phenotypic characterization of individuals with 30-40 CAG repeats in the HD gene reveals HD cases with 36 repeats and apparently normal elderly individuals with 36-39 repeats. *Am J Hum Genet* 59:16-22.

80. Samii A, Nutt JG, Ransom BR (2004) Parkinson's disease. *The Lancet* 363:1783-1793.

81. Sapp E, Schwarz C, Chase K, Bhide PG, Young AB, Penney J, Vonsattel JP, Aronin N, Difiglia M (1997) Huntingtin localization in brains of normal and Huntington's disease patients. *Ann Neurology* 42:604-612.

82. Sawa A (2001) Mechanisms for neuronal cell death and dysfunction in Huntington's disease: pathological cross-talk between the nucleus and the mitochondria? *J Mol Med* 79: 375-381.

83. Schilling G, Becher MW, Sharp AH, Jinnah HA, Duan K, Kotzuk JA, Slunt HH, Ratovitski T, Cooper JK, Jenkins NA, Copeland NG, Price DL, Ross CA, and Borchelt DR (1999) Intranuclear inclusions and neuritic aggregates in transgenic mice expressing a mutant N-terminal fragment of huntingtin. *Hum Mol Genet* 8:397–407.

84. Schilling G, Coonfield ML, Ross CA, and Borchelt DR (2001) Coenzyme Q10 and remacemide hydrochloride ameliorate motor deficits in a Huntington's disease transgenic mouse model. *Neurosci Lett* 315:149–153.

85. Schilling G, Jinnah HA, Gonzales V, Coonfield ML, Kim Y, Wood JD, Price DL, Li XJ, Jenkins N, Copeland N, Moran T, Ross CA, and Borchelt DR (2001) Distinct behavioral and neuropathological abnormalities in transgenic mouse models of HD and DRPLA. *Neurobiol Dis* 8:405–418.

86. Schwarcz R, Whetsell WO, Mangano KM (1983) Quinolinic acid an endogenous metabolite that produces axon-sparing lesion in rat brain. *Science* 219:316-318.

87. Sekimata M, Takahashi A, Murakami-Sekimata A, and Homma Y (2001) Involvement of a novel zinc finger protein, MIZF, in transcriptional repression by interacting with a methyl-CpG-binding protein, MBD2. *J Biol Chem* 276:42632–42638.

88. Shimohata T, Nakajima T, Yamada M, Uchida C, Onodera O, Naruse S, Kimura T, Koide R, Nozaki K, Sano Y, Ishiguro H, Sakoe K, Ooshima T, Sato A, Ikeuchi T, Oyake M, Sato T, Aoyagi Y, Hozumi I, Nagatsu T, Takiyama Y, Nishizawa M, Goto J, Kanazawa I, Davidson I, Ranese N, Takahashi H, and Tsuji S (2000) Expanded polyglutamine stretches interact with TAFII130, interfering with CREB-dependent transcription. *Nat Genet* 26:29–36.

89. Singhrao SK, Neal JW, Morgan BP and Gasque P (1999) Increased complement biosynthesis by microglia and complement activation on neurons in Huntington's disease. *Exp Neurol* 159: 362–376.

90. Slow EJ, van Raamsdonk J, Rogers D, Coleman SH, Graham RK, Deng Y, Oh R, Bissada N, Hossain SM, Yang YZ, Li XJ, Simpson EM, Gutekunst CA, Leavitt BR, Hayden MR. (2003) Selective striatal neuronal loss in a YAC128 mouse model of Huntington's disease. *Hum Mol Genet* 12:1555-1567.

91. Steffan JS, Bodai L, Pallos J, Poelman M, McCampbell A, Apostol BL, Kazantsev A, Schmidt E, Zhu YZ, Greenwald M, Kurokawa R, Housman DE, Jackson GR, Marsh JL, Thompson LM (2001) Histone deacetylase inhibitors arrest polyglutamine-dependent neurodegeneration in Drosophila. *Nature* 413:739-743.

92. Strachan T, Read AP (1996) Human molecular genetics. Chapter 10: Mutation and instability of human DNA, BIOS Scientific Publishers Limited, Oxford.

93. Sun Y, Savanenin A, Reddy PH, Liu YF (2001) Polyglutamin-expanded huntingtin promotes sensitization of *N*-methyl-*D*-aspartate receptors via post-synaptic density 95. *J Biol Chem* 276: 24713-24718.

94. Tabrizi SJ, Workman J, Hart PE, Mangiarini L, Mahal A, Bates G, Cooper JM and Schapira AH (2000) Mitochondrial dysfunction and free radical damage in the Huntington R6/2 transgenic mouse. *Ann Neurol* 47: 80–86.

95. Taylor JP, Taye AA, Campbell C, Kazemi-Esfarjani P, Fischbeck KH, and Min KT (2003) Aberrant histone acetylation, altered transcription, and retinal degeneration in a Drosophila model of polyglutamine disease are rescued by CREB-binding protein. *Genes Dev* 17:1463–1468.

96. Tipton KF, Singer TP (1993) Advances in our understanding of the mechanisms of the neurotoxicity of MPTP and related compounds. *J Neurochem* 61:1191-1206.

97. Vécsei L, Beal MF (1991) Comparative behavioral and neurochemical studies with striatal kainic acid- or quinolinic acid-lesioned rats. *Pharmacol Biochem Behav* 39:473-478.

98. Vécsei L, Beal MF (1996) Huntington's disease, behavioral disturbances, and kynurenines: preclinical findings and therapeutic perspectives. *Biol Psychiatry* 39:1061-1063.

99. Vécsei L, Dibo Gy, Kiss Cs (1998) Neurotoxins and neurodegenerative disorders. *Neurotoxicology* 19:511-514.

100. Walton MR, Dragunow I (2000) Is CREB a key to neuronal survival? *Trends Neurosci* 23:48-53.

101. Warrell RP Jr, He LZ, Richon V, Calleja E, Pandolfi PP (1998) Therapeutic targeting of transcription in acute promyelocytic leukemia by use of an inhibitor of histone deacetylase. *J Natl Cancer Inst* 90:1621-1625.

102. Wyttenbach A, Swartz J, Kita H, Thykjaer T, Carmichael J, Bradley J, Brown R, Maxwell M, Schapira A, Orntoft TF, Kato K, Rubinsztein DC (2001) Polyglutamine expansions cause decreased CREB-mediated transcription and early gene expression changes prior to cell death in an inducible cell model of Huntington's disease. *Hum Mol Genet* 10:1829-1845.

103. Wyttenbach A, Sauvageot O, Carmichael J, Diaz-Latoud C, Arrigo AP and Rubinsztein DC (2002) Heat shock protein 27 prevents cellular polyglutamine toxicity and suppresses the increase of reactive oxygen species caused by huntingtin. *Hum Mol Genet* 11: 1137–1151.

104. Yu ZX, Li SH, Evans J, Pillarisetti A, Li H, and Li XJ (2003) Mutant huntingtin causes context-dependent neurodegeneration in mice with Huntington's disease. *J Neurosci* 23, 2193–2202.

105. Zhang Y, and Reinberg D (2001) Transcription regulation by histone methylation: interplay between different covalent modifications of the core histone tails. *Genes Dev* 15:2343–2360.

106. Zeitlin S, Liu JP, Chapman DL, Papaioannou VE, Efstratiadis A. (1995) Increased apoptosis and early embryonic lethality in mice nullizygous for the Huntington's disease gene homolog. *Nat Genet* 11:155-163.

107. Zeron MM, Chen N, Moshaver A, Lee AT, Wellington CL, Hayden MR, Raymond LA (2001) Mutant huntingtin enhances excitotoxic cell death. *Mol Cell Neurosci* 17:41-53.

108. Zeron MM, Hansson O, Chen N, Wellington CL, Leavitt BR, Brundin P, Hayden MR and Raymond LA (2002) Increased sensitivity to N-methyl-D-aspartate receptor-mediated excitotoxicity in a mouse model of Huntington's disease. *Neuron* 33: 849–860.

109. Zuccato C, Ciammola A, Rigamonti D, Leavitt BR, Goffredo D, Conti L, MacDonald ME, Friedlander RM, Silani V, Hayden MR, Timmusk T, Sipione S, Cattaneo E.(2001) Loss of Huntingtin-mediated BDNF gene transcription in Huntington's disease. *Science* 293:493-498.